

Toward Understanding In-context vs. In-weight Learning

Bryan Chan^{1*}, Xinyi Chen^{2*}, András György², Dale Schuurmans^{1,2}

{bryan.chan}@ualberta.ca,
{xinyic, agyorgy, schuurmans}@google.com
¹University of Alberta ²Google DeepMind

Abstract

It has recently been demonstrated empirically that in-context learning emerges in transformers when certain distributional properties are present in the training data, but this ability can also diminish upon further training. We provide a new theoretical understanding of these phenomena by identifying simplified distributional properties that give rise to the emergence and eventual disappearance of in-context learning. We do so by first analyzing a simplified model that uses a gating mechanism to choose between an in-weight and an in-context predictor. Through a combination of a generalization error and regret analysis we identify conditions where in-context and in-weight learning emerge. These theoretical findings are then corroborated experimentally by comparing the behaviour of a full transformer on the simplified distributions to that of the stylized model, demonstrating aligned results. We then extend the study to a full large language model, showing how fine-tuning on various collections of natural language prompts can elicit similar in-context and in-weight learning behaviour.

1 Introduction

In-context learning (ICL) is an interesting and useful property exhibited by large language models (LLMs), wherein a model is able to successfully learn and generalize from new information given in its input, without ever having seen related data during training. Radford et al. (2019) and Brown et al. (2020) were among the first to demonstrate the in-context learning capability of large-language models. Since then, numerous empirical studies have attempted to understand the emergence of ICL in LLMs (Olsson et al., 2022; Wei et al., 2023; Agarwal et al., 2024; Shi et al., 2024). However, ICL is not limited to natural language processing (NLP), and many synthetic settings have been constructed to better understand this phenomenon (Garg et al., 2022; Akyürek et al., 2023; Von Oswald et al., 2023; Gupta et al., 2023; Edelman et al., 2024a; Wu et al., 2024; Zhang et al., 2024a).

A recent line of work (Chan et al., 2022a; Reddy, 2023; Singh et al., 2023) has explored the emergence of ICL through the lens of data-distributional properties. In particular, Chan et al. (2022a) first proposed the importance of common and rare classes as driving in-context learning and in-weight learning (IWL). Both Chan et al. (2022a) and Reddy (2023) empirically identified that ICL can emerge in a transformer model (Vaswani et al., 2017) when there is a large within-class variation and a large number of classes. Chan et al. (2022a,b) further observed that both ICL and IWL can emerge simultaneously when the distribution over classes is Zipfian, while Singh et al. (2023) subsequently noticed that ICL can become transient in an asymptotic training regime.

The work in this paper is inspired by a similar distributional perspective, but we investigate in greater depth how the distributional properties of the data affect the ability of a transformer model to learn and implement in-weight (IW) and in-context (IC) predictors over different parts of the input space. In particular, we provide insights on the emergence of ICL in synthetic settings with theory and experiments, and bridge the gap to practice by demonstrating that similar phenomena continue to hold in a simple NLP task with a real LLM, Gemini Nano 1 (Gemini Team, Google, 2023).

*Equal contribution.

Contributions. We present a simple theoretical model in which ICL both emerges and becomes transient in the infinite data regime, demonstrating that very simple properties of the training distribution can lead to these phenomena. In particular, following the common vs. rare classes distribution of Chan et al. (2022a), our model requires two types of data: (i) data where similar observations frequently appear in the training set—this type of data will induce in-weight learning; and (ii) a large number of diverse data points, where each sample is predictable from the context, but each appears rarely so that reliable IW learning cannot be achieved—this type of data will induce IC learning.

Through a combination of a generalization error and regret bound analysis, we identify conditions where in-context and in-weight learning emerge. In particular, our theoretical model shows that the presence of type (i) data (which we refer to as *in-weight* data) induces in-weight learning and the presence of type (ii) data (referred to as *in-context* data) leads to in-context learning. This is consistent with the empirical findings of Chan et al. (2022a): When a sufficient number of in-context data samples are present, such as samples from rare classes, in-context learning emerges—the Zipfian distribution provides a good balance between in-context and in-weight data. When the model is trained over more samples, the samples from rare classes (or in-context data) accumulate and the model learns in-weight after observing sufficiently many samples from a given class. In other words, the in-context data becomes in-weight data, and the lack of in-context data encourages the model to rather use in-weight prediction than in-context, resulting in the reduction of in-context learning, which explains the findings of Singh et al. (2023).

We demonstrate empirically that training transformers on synthetic and Omniglot data drawn from the stylized distribution in our theoretical model follows the predictions of the developed theory. Finally, to bridge the gap from theory to practice, we further show that fine-tuning a full large language model to memorize certain data can result in a reduction of its in-context learning ability.

Additional related work. We do not investigate how transformers learn circuits that can perform ICL. While such ability can evidently emerge from a vast amount of in-context training data and a sufficiently expressive architecture (function class), several works have investigated mechanistically how transformers can realize ICL (Garg et al., 2022; Olsson et al., 2022; Xie et al., 2022; Akyürek et al., 2023; Hendel et al., 2023; Abernethy et al., 2024; Singh et al., 2024). In particular, Garg et al. (2022) have demonstrated transformers can in-context learn simple regression tasks and Akyürek et al. (2023) mathematically constructed instances in which transformers can implement gradient descent and closed-form regression. Xie et al. (2022) cast ICL as implicit Bayesian inference and have shown that ICL is optimal when provided infinite examples with distinguishable prompts. Hendel et al. (2023) have empirically demonstrated that the transformer can compress context into a task vector and direct the output of the query. Chen et al. (2024) and Sanford et al. (2024) focus on understanding the formation and the limitations of induction heads. These works generally enforce ICL by constructing context sequences, each corresponding to a new task. By contrast, we investigate how ICL can emerge with context sequences of only a single task.

A number of recent works have contributed to the theoretical study of ICL. Bai et al. (2023) show that transformers can implement many machine learning algorithms in-context, such as gradient descent and least squares, and furthermore they can perform in-context algorithm selection. Authors also show excess loss guarantees for pretraining the transformer to perform ICL on polynomial number of sequences. Li et al. (2023) formalizes ICL as an algorithm learning problem, where during pretraining the transformer learns a prediction function from the training sequences. They further provide generalization bounds from a multi-task learning perspective using algorithmic stability. Nichani et al. (2024) study ICL by focusing on the ability of transformers to learn causal structures. They show gradient descent on a simplified two-layer transformer can learn causal structures when the causal graph is a tree, and when the training sequences are generated by a Markov chain, the model can learn an induction head. Edelman et al. (2024b) also study how transformers learn induction heads in this setting, focusing on the multi-phase learning process. Zhang et al. (2024b) study the learning dynamics of training a single linear attention layer with gradient flow on linear regression tasks. They show that with random initialization, gradient flow on this architecture can in-context learn the class of linear predictors. Wu et al. (2024) further studies the generalization error under a similar setting, and characterize how many tasks is needed to pretrain the model. They also show that the learned solution is competitive with the Bayes optimal predictor under certain conditions. Our theoretical work differs in that we focus on the selection of in-weight learning and in-context learning based on their corresponding test errors.

2 Theoretical analysis

In this section we present our theoretical model. In essence, we consider a bi-level model that learns a “memorizing” in-weight predictor g as well as an in-context predictor h , and for every input \tilde{x} it follows the prediction of the submodel that is expected to be better for that particular data point. Naturally, g can be learned with high fidelity in parts of the input space where there is enough training data, while h can be effective anywhere where the context is useful. The final behavior of the model then will depend on the expected accuracy of g and h for a given input. In the rest of this section we formalize this approach in the setting of tabular classification problems.

2.1 Setting

Let $\mathcal{X} \subset \mathbb{R}^d$ be the finite space of inputs,¹ C be the number of classes, and let the space of labels be Δ_C , the C -dimensional simplex. We have access to a training dataset S of N examples, where in addition to the usual (input, label) pairs in a classification problem, each example has a context consisting of L extra (input, label) pairs: $S = \{(x_i^1, y_i^1, x_i^2, y_i^2, \dots, x_i^L, y_i^L, x_i), y_i\}_{i=1}^N$. Let $\tilde{x}_i := (x_i^1, y_i^1, x_i^2, y_i^2, \dots, x_i^L, y_i^L, x_i)$ denote the i -th training example, and $\tilde{\mathcal{X}} = (\mathcal{X} \times \Delta_C)^L \times \mathcal{X}$ be the space of examples with context. Suppose (\tilde{x}_i, y_i) are drawn from a ground-truth distribution \mathcal{D} ; during training the task is to predict y_i given \tilde{x}_i , while the final goal is to minimize the prediction error for a new sample (\tilde{x}, y) sampled independently from \mathcal{D} where $\tilde{x} = (x^1, y^1, x^2, y^2, \dots, x^L, y^L, x)$.

In the latter, the prediction error is measured by the loss function $\ell : \Delta_C \times \Delta_C \rightarrow [0, 1]$, where $\ell(\hat{y}, y)$ is the loss of the prediction \hat{y} given the label y . Since one can always scale the loss, we assume the loss is bounded by 1 without loss of generality. In addition, we assume it is convex in its first argument. This condition is satisfied by common losses such as cross-entropy and squared loss.

Data-generating process. We consider the setting of inputs with label noise: there exists a mapping $y^* : \mathcal{X} \rightarrow \Delta_C$, such that the true label for input x is $y^*(x)$. When we sample x in the context or as the query, we sample $y = e_i$, the i -th standard basis vector, with probability $y^*(x)_i$.

Predictors. Below, we formalize the two classes for learning: the in-weight learning (IWL) class \mathcal{G} , and the in-context learning (ICL) class \mathcal{H} . The *IWL class* of functions \mathcal{G} uses *only the query*, and is a tabular function class: for each $x \in \mathcal{X}$, g can learn a separate mapping from x to Δ_C . We denote $\mathcal{G} = \{g : \tilde{\mathcal{X}} \rightarrow \Delta_C, g(\tilde{x}; w) = g(x; w) = w(x) \in \Delta_C, w \in \Delta_C^{|\mathcal{X}|}\}$. The *ICL class* of functions \mathcal{H} uses *only labels in the context* to make a prediction, and let it be parameterized by u belonging to some set \mathcal{W} . Inspired by the induction head (Olsson et al., 2022), a circuit that learns to copy tokens in the context to the output, we design \mathcal{H} consisting of functions that output a convex combination of the labels in the context. In addition, we mix in uniform distribution to ensure numerical stability. Let $h' : \tilde{\mathcal{X}} \times \mathcal{W} \rightarrow \Delta_L$ be a function that outputs weights for a convex combination (a distribution) given an example, and let $\mathcal{H} = \{h : \tilde{\mathcal{X}} \rightarrow \Delta_C, h(\tilde{x}; u) = \epsilon \mathbf{1} + (1 - C\epsilon) \sum_{l=1}^L h'(\tilde{x}; u)_l y_l, u \in \mathcal{W}\}$.

Simple model. We design a model that selects among the in-weight and in-context learners by a function α , which can take a different value in $[0, 1]$ for each $\tilde{x} \in \tilde{\mathcal{X}}$. We analyze the following simplified model f to study the emergence of in-context vs. in-weight learning: for each \tilde{x} , $f(\tilde{x}; \alpha, w, u) = \alpha(\tilde{x})g(\tilde{x}; w) + (1 - \alpha(\tilde{x}))h(\tilde{x}; u)$.

2.2 Selection by test error

Previous empirical observations show that ICL emerges when the data distribution has a long tail with many rare classes (Chan et al., 2022a). We investigate the hypothesis that ICL emerges because in-weight learning has large error on classes that have few samples in the training dataset. We first quantify the generalization error of the in-weight learner. Then, we consider a more explicit class of in-context learners and give upper and lower bounds on the errors of the IC predictor.

We start by stating a usual generalization bound (Boucheron et al., 2012) for a learning algorithm (proofs are given in Appendix A for completeness).

¹The finiteness of \mathcal{X} is only assumed to simplify the exposition; the results can easily be extended to a continuous input space \mathcal{X} .

Proposition 1. Suppose we have N examples in S drawn independently from the data distribution \mathcal{D} , and let S_x denote the subset of S with x as the query in the example. Let $|S_x| = N_x$. Let \hat{g} be the empirical risk minimizer of S , i.e. for any x , $\hat{g}(x) = \arg \min_{\hat{y} \in \Delta_C} \frac{1}{N_x} \sum_{(\tilde{x}, y) \in S_x} \ell(\hat{y}, y)$. Let $G_\infty \geq \|\nabla \ell(\cdot, y)\|_\infty$ be an upper bound on the infinity norm of the gradients, where $G_\infty \geq 1$. Then with probability at least $1 - \delta$, for any $x \in \mathcal{X}$, the risk of $\hat{g}(x)$ satisfies

$$\mathbb{E}_y[\ell(\hat{g}(x), y)] \leq \min_{y^* \in \Delta_C} \mathbb{E}_y[\ell(y^*, y)] + 6G_\infty \sqrt{\log(2|\mathcal{X}|C/\delta)/N_x}.$$

The optimal risk satisfies $\min_{y^* \in \Delta_C} \mathbb{E}_y[\ell(y^*, y)] \leq \mathbb{E}_y[\ell(y^*(x), y)]$, where the right hand side can be seen as the ‘‘variance’’ of y .

Inspired by the induction head and attention mechanism in transformers (Olsson et al., 2022), we consider the following function class for in-context learning:

$$\mathcal{H} = \left\{ h(\tilde{x}) = \epsilon \mathbf{1} + (1 - C\epsilon) \sum_{l=1}^L \frac{\exp(-\|x^l - x\|_A)}{\sum_{j=1}^L \exp(-\|x^j - x\|_A)} y^l, \|A\| \leq B \right\},$$

where A is a $d \times d$ positive semidefinite matrix, $\|A\|$ denotes the spectral norm of A , and $\|x\|_A = \sqrt{x^\top A x}$ for any $x \in \mathbb{R}^d$. The idea is that a function $h \in \mathcal{H}$ implements a simplified induction head, averaging the label predictions y_l for all context vectors x_l weighted by a softmax depending on the similarity of x_l and the query x . If the context contains *irrelevant* labels, that is, labels $y_l \neq y$ for some $l \in [L]$, the prediction will be noisy, as shown in the next proposition.

Proposition 2. Given an example sequence \tilde{x} , let y be the label, and k be the number of irrelevant labels in the context. Suppose for all $x \in \mathcal{X}$, $\|x\| \leq 1$, then the prediction of any $h \in \mathcal{H}$ satisfies

$$\frac{2k(1 - \epsilon C)}{k + (L - k) \exp(2\sqrt{B})} + 2\epsilon(C - 1) \leq \|h(\tilde{x}) - y\|_1 \leq \frac{2k(1 - \epsilon C)}{L} + 2\epsilon(C - 1).$$

Specializing $\ell(\hat{y}, y)$ to cross-entropy loss $CE(\hat{y}, y) = \sum_{c \in C} -y_c \log \hat{y}_c$, we obtain the following.

Corollary 1. Assume the labels y are one-hot (deterministic). Let \tilde{x} be an example sequence. If \tilde{x} does not contain a relevant label, then $CE(h(\tilde{x}), y) = \log \frac{1}{\epsilon}$. If \tilde{x} contains k irrelevant labels, then

$$\frac{k(1 - \epsilon C)}{k + (L - k) \exp(2\sqrt{B})} + \epsilon(C - 1) \leq CE(h(\tilde{x}), y) \leq -\log \left((1 - \epsilon C) \frac{L - k}{L} + \epsilon \right).$$

The guarantees above show that the test error of the IW predictor converges to that of the optimal predictor at a rate of $O(1/\sqrt{N_x})$, while the IC predictor has a minimum test error depending on the number of irrelevant labels. In the case where the true labels $y^*(x)$ have low variance, and the best IW predictor achieves lower risk than the IC predictor, the IW predictor will eventually be more accurate than the IC predictor given enough samples.

We plot the bounds in Figure 1. Indeed, with few samples, the loss of the IC predictor can be smaller than that of the IW predictor. However, the IW predictor eventually converges to a solution with smaller error after seeing many examples with the same query. We can consider an oracle algorithm that selects between the learned IW predictor \hat{g} and IC predictor \hat{h} based on their test error (i.e., how they would perform on new data), and predicts

$$f(\tilde{x}) = \alpha(\tilde{x})\hat{g}(x) + (1 - \alpha(\tilde{x}))\hat{h}(\tilde{x}), \quad \text{where} \quad \alpha(\tilde{x}) = \mathbb{I} \left\{ \mathbb{E}_y[\ell(\hat{g}(x), y)] \leq \mathbb{E}_y[\ell(\hat{h}(\tilde{x}), y)] \right\}$$

is the indicator function whether the expected test error of \hat{g} does not exceed that of \hat{h} for a particular input \tilde{x} . Under this algorithm, ICL will first emerge on rare classes, and will eventually be replaced by the IW predictor on those classes. This phenomenon is consistent with the empirical observation that in-context learning emerges with rare classes in the training data, and is transient after training for more steps with freshly-sampled data (Chan et al., 2022a; Singh et al., 2023).

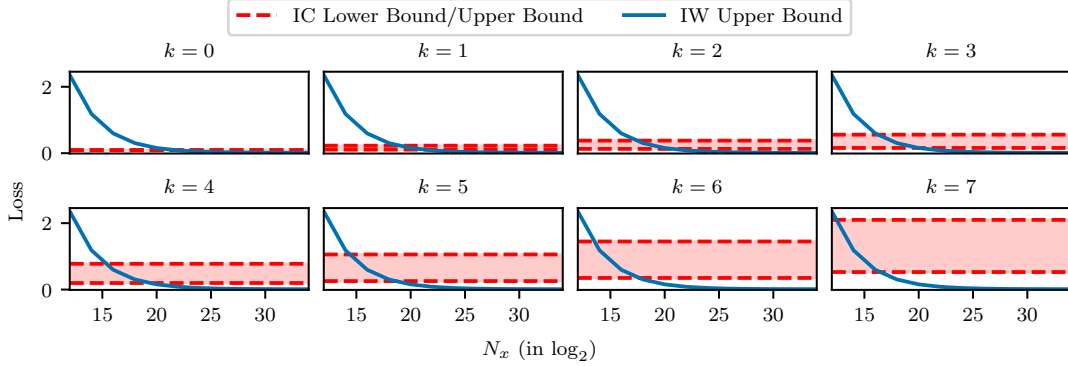


Figure 1: The theoretical error bounds of IC and IW predictors. We set $L = 8$, $\epsilon = 0.001$, $B = 1$, $C = 10$, $\Delta_C = [0.999, 0.001/9, \dots, 0.001/9]$, and Big- O constant of the IW risk to be 20. As the number of irrelevant contexts, k , increases the lower bound of IC error also increases, whereas where the number of samples, N_x , increases the upper bound of the IW error decreases. Consequently one can expect ICL to be transient as we observe more samples.

2.3 Learning to use in-context vs. in-weight learning

In practice, the model does not observe the test error during training. Here we attempt to bridge the gap between the oracle algorithm and the behavior of the simple model when f is trained using gradient-based methods. Consider the usual sequential training procedure: for each sample \tilde{x}_t , $t = 1, \dots, N$, the model predicts $f_t(\tilde{x}_t; \alpha_t) = \alpha_t(\tilde{x}_t)g(\tilde{x}_t; w_t) + (1 - \alpha_t(\tilde{x}_t))h(\tilde{x}_t; u_t)$, and the parameters w_{t+1} , u_{t+1} , α_{t+1} are updated based on the observed loss $\ell_t(f_t(\tilde{x}_t)) = \ell(f_t(\tilde{x}_t), y_t)$.

The parameters w_t , u_t , α_t are usually updated using some gradient-based method \mathcal{A}_f . Apart from converging to a local optimum of the loss function under technical assumptions (e.g., convexity of the loss function, see, e.g., Zinkevich, 2003; Hazan, 2023), such algorithms often guarantee that their regret grows only sublinearly in N , where the regret of algorithm \mathcal{A}_f is defined as

$$\text{Regret}_N(\mathcal{A}_f) = \sum_{t=1}^N \ell(f_t(\tilde{x}_t; \alpha_t), y_t) - \min_{w, u, \alpha} \sum_{t=1}^N \ell(f(\tilde{x}_t; w, u, \alpha), y_t),$$

the excess loss of the online updated parameter sequence $(w_t, u_t, \alpha_t)_{t=1}^N$ relative to that of the optimal predictor selected in hindsight (where $f(\cdot, w, u, \alpha) = \alpha(\cdot)g(\cdot; w) + (1 - \alpha(\cdot))h(\cdot; u)$). Sublinear regret means that the average loss of the algorithm converges to the loss of the optimal predictor; algorithms with this property are called *no-regret* algorithms (as the average regret converges to zero). Note that when minimizing the regret, the parameters used to predict at time step t are computed based on the observed data $(\tilde{x}_1, y_1), \dots, (\tilde{x}_{t-1}, y_{t-1})$, and are evaluated on a new data point (\tilde{x}_t, y_t) ; hence the choice of α_t is evaluated on new data, similarly to our recommendation at the end of the previous subsection, where the choice between the IW and IC predictors should be based on their performance on new, unseen data, that is, the test error.

For simplicity, we consider a bi-level parameter update procedure shown in Algorithm 1. Since g is tabular, it can implement the optimal fixed predictor for each input x , and hence in the regret definition we can use $g(\cdot; w^*)$ (where w^* is the optimal parameter for g). In the following proposition we show that the regret of Algorithm 1 is bounded by the regret of learning α and g . If \mathcal{A}_α and \mathcal{A}_g are no-regret algorithms, Algorithm 1 has sublinear regret. Moreover, observe that under the linear losses m_t , the best-in-hindsight α chooses the predictor with the lower total loss for each \tilde{x} . Indeed, denote α^* to be the best α in hindsight given the losses m_t , it has the following explicit form:

$$\alpha^*(\tilde{x}) = 1 \text{ if } \sum_{t: \tilde{x}_t = \tilde{x}} \ell_t(g(\tilde{x}_t; w_t)) - \ell_t(h(\tilde{x}_t; u_t)) < 0, \quad \alpha^*(\tilde{x}) = 0 \text{ otherwise}$$

Algorithm 1 Bi-level update

Input: horizon N , no-regret learner \mathcal{A}_α , \mathcal{A}_g for g , and \mathcal{A}_h for h .

for $t = 1$ to N **do**

 Receive example \tilde{x}_t , predict with $f_t(\tilde{x}_t; \alpha_t) = \alpha_t(\tilde{x}_t)g(\tilde{x}_t; w_t) + (1 - \alpha_t(\tilde{x}_t))h(\tilde{x}_t; u_t)$

 Observe losses $\ell_t(f_t(\tilde{x}_t; \alpha_t))$, $\ell_t(g(\tilde{x}_t; w_t))$, $\ell_t(h(\tilde{x}_t; u_t))$

 Update $w_{t+1} = \mathcal{A}_g(\ell_1(g(\tilde{x}_1; w_1)), \dots, \ell_t(g(\tilde{x}_t; w_t)))$

 Update $u_{t+1} = \mathcal{A}_h(\ell_1(h(\tilde{x}_1; u_1)), \dots, \ell_t(h(\tilde{x}_t; u_t)))$

 Define $m_t(\alpha_t) = \alpha_t(\tilde{x}_t)(\ell_t(g(\tilde{x}_t; w_t)) - \ell_t(h(\tilde{x}_t; u_t)))$

 Update $\alpha_{t+1} = \mathcal{A}_\alpha(m_1, \dots, m_t)$

end for

Proposition 3. Let x_t denote the query at time t , let $\text{Regret}_N(\mathcal{A}_g) = \sum_{t=1}^N \ell(g(x_t; w_t), y_t) - \sum_{t=1}^N \ell(g(x_t; w^*), y_t)$ be the regret of learning g , and $\text{Regret}_N(\mathcal{A}_\alpha) = \sum_{t=1}^N m_t(\alpha_t) - m_t(\alpha^*)$ be the regret of learning α . Algorithm 1 satisfies

$$\sum_{t=1}^N \ell(f_t(\tilde{x}_t; \alpha_t), y_t) - \sum_{t=1}^N \ell(g(\tilde{x}_t; w^*), y_t) \leq \text{Regret}_N(\mathcal{A}_\alpha) + \text{Regret}_N(\mathcal{A}_g).$$

Since the problem of learning α^* is linear, common gradient-based algorithms have sublinear regret. For example, both the exponentiated gradient and the AdaGrad method with a diagonal preconditioner achieves $O(\sqrt{KN})$ regret, where K is the number of distinct examples seen during the learning process (see, e.g., Cesa-Bianchi and Lugosi, 2006; Hazan, 2023). Further, since g learns a separate (independent) predictor for each x , and ℓ is convex, the problem of learning $g(x)$ is convex. Many regret-minimizing algorithms, including gradient descent, has $O(\sqrt{K'N})$ regret in this setting, where K' is the number of distinct queries observed. In this case, we have overall sublinear regret against the best in-weight learner g^* . This guarantee implies that on average, our loss converges to that of the best in-weight predictor in hindsight.

Suppose the examples $\{(\tilde{x}_t, y_t)\}_{t=1}^N$ are drawn i.i.d. from the population distribution. Then by online-to-batch conversion (Cesa-Bianchi et al., 2001), the expectation of the average loss of $g(\cdot; w_t)$ in Algorithm 1 exhibits similar behavior as the generalization-error guarantee. We give a standard result below. If we consider the same class of ICL predictors, they also will have a positive minimum loss for each ℓ_t as in the previous section.

Proposition 4. Fix $x \in \mathcal{X}$. Suppose $\{(\tilde{x}_t, y_t)\}_{t=1}^N$ are drawn i.i.d. from \mathcal{D} , where y is drawn i.i.d. given the query x . Let N_x be the number of examples with x as the query, then

$$\frac{1}{N_x} \mathbb{E}_{y_t: x_t=x} \left[\sum_{t: x_t=x} \ell_t(g(x; w_t)) \right] \leq \min_w \mathbb{E}_y [\ell(g(x; w), y)] + \frac{1}{N_x} \mathbb{E} [\text{Regret}_{N_x}(\mathcal{A}_g(x))],$$

where $\text{Regret}_{N_x}(\mathcal{A}_g(x))$ is the regret of \mathcal{A}_g on the input x , learned over N_x time steps.

In other words, although the model in practice does not directly observe the test error during training, the training samples observed at each training iteration can be viewed as a “test” sample, its loss provides a quantity similar to that of the test error.

The above results show that as long as \mathcal{A}_g and \mathcal{A}_α are no-regret algorithms (which are satisfied in this setting by simple gradient descent, see, e.g., Zinkevich, 2003), the performance of the final predictor approximates well the performance of the optimal predictor, and α_N approximates well α^* , implying that the learned model will select IC on IW prediction depending on their performance. This shows that the unrealistic step of choosing between an IC or IW predictor based on their (unknown) test error, as suggested at the end of Section 2.2, can be replaced by a decision rule learned during training using an algorithm similar to gradient descent. Note that we have not included the complexity of learning the IC predictor h . Nevertheless, we demonstrate experimentally in the next section that the predictions drawn from our simple models are valid in many practical scenarios.

3 Experiments

In this section we demonstrate through various experiments that our simple theoretical model is predictive and can help explain the relationship between ICL and IWL in practical settings.

3.1 Synthetic classification

In this section we consider a synthetic classification task and investigate how the errors of IC and IW predictors can inform whether a transformer trained end-to-end will exhibit ICL capabilities. How different parameters impact the emergence and transient of ICL are explored in Appendix B.1.

Data. We consider a classification problem with an imbalanced data distribution, where there are high- and low-frequency (i.e., common and rare) classes. Let C_H and C_L denote their label sets, respectively, and let $C = C_H \cup C_L$. Each sample is generated by first selecting a target query-response pair (x, y) then generating the accompanying context sequence. An input-output pair (x, y) is sampled from a joint distribution $p(x, y) = p(x|y)p(y)$, which we refer to as the *base distribution*. First we sample a label from the label distribution $p(y)$ which is a mixture of uniform distributions over the high- and low-frequency classes C_H and C_L , with weights p_{high} and $p_{low} = 1 - p_{high}$: that is, $p(y) = p_{high}/|C_H|$ if $y \in C_H$ and $p(y) = p_{low}/|C_L|$ if $y \in C_L$; we assume that $p_{high} \gg p_{low} = 1 - p_{high}$. The distribution of queries for class $y \in C$ is parametrized by a prototype vector x_y from the d -dimensional unit sphere; for each $y \in C$, x_y is sampled uniformly from the unit sphere and is a fixed parameter of the distribution $p(x|y)$. Then x is obtained by normalizing a perturbed version of the corresponding prototype vector x_y , where the perturbation is Gaussian; formally, $x = (x_y + \varepsilon)/\|x_y + \varepsilon\|_2$, where $\varepsilon \sim \mathcal{N}(0, \Sigma)$. To sample the context to a query-target pair (x, y) , first with probability $p_{relevant}$ we decide if the context is *relevant* to (x, y) , that is, if it should contain at least one query-target pair from the same class y . Then the context is obtained by sampling L input-output pairs from p independently under the condition that the resulting L -tuple contains a class- y sample if and only if the context should be relevant.

Experimental setup. We conduct experiments by training a transformer (GPT) end-to-end (Radford, 2018). The models consist of two transformer decoder layers, each with a single attention head and processes 64-dimensional embeddings. Both the input and output tokenizers are linear projections, where the former is the identity matrix. For prediction we take the last token output from the last transformer block and feed it into a linear layer followed by a softmax. To probe the difficulty of IWL and ICL, we separately train two transformers for these two settings by using data with $p_{relevant} = 0.0$ and $p_{relevant} = 1.0$; we refer to these models as the *IW and IC predictors*, respectively. A generic model trained on data with $p_{high} = 0.9$ is referred to as the *transformer*. Unless specified otherwise, all models are trained using cross-entropy loss for 50K gradient updates with batch size of 32. We set $C_H = \{0, \dots, 4\}$ and $C_L = \{5, \dots, 9\}$, and set the input dimension $d = 64$ with $\Sigma = \sigma^2 I_d$ where $\sigma = 0.2$ and I_d is the $d \times d$ identity matrix. Furthermore, we fix the context length $L = 1$, the probability of sampling high-frequency classes $p_{high} = 0.9$, and vary the number of total samples $N = \{2^6, 2^8, \dots, 2^{20}\}$. We repeat each experiment five times, and in the figures we show confidence intervals of width 1 standard deviation.

Evaluation. To evaluate whether the trained models exhibit IWL or ICL, we evaluate the trained models on *in-base distribution* (IBD) and *out-of-base distribution* (OOBD). The OOBD data is obtained from the base distribution data by cyclically shifting the labels of the high-frequency and low-frequency classes respectively. Since the labels in the in-base and out-of-base distributions are different for each query, any purely IW predictor trained on the base distribution is doomed to fail on OOBD data, while the latter can be predicted IC if the context is relevant. A model that exhibits purely IWL will result in low error IBD regardless of context relevance, but will result in high error OOBD. On the other hand, a model that exhibits purely ICL will result in low error on relevant contexts, but will result in high error on irrelevant contexts.

Main results. Our first experiments aim to identify conditions in which ICL emerges and/or is transient. Figure 2 shows that slight input perturbation can elicit ICL capabilities from the transformer. As the dataset size N increases,

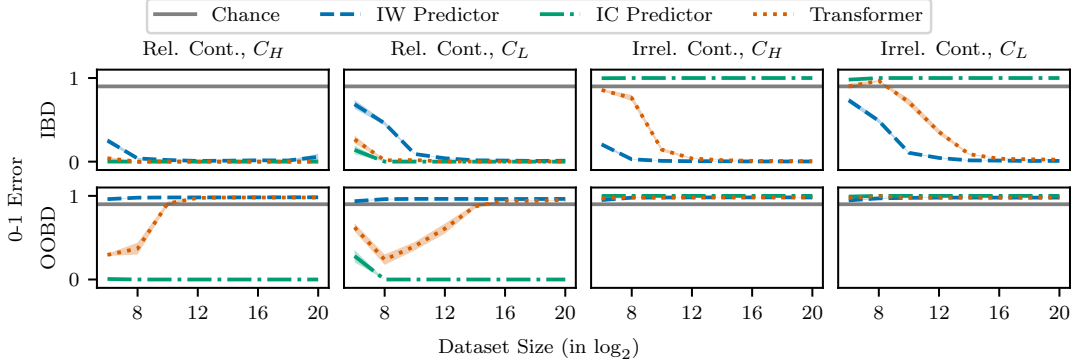


Figure 2: 0-1 validation errors of the IC predictor, IW predictor, and transformer as a function of training set size N on the synthetic data, over five seeds. $L = 1$, $p_{high} = 0.9$, $p_{relevant} = 0.9$ and $\sigma = 0.2$. The columns correspond to test data with relevant/irrelevant context, and classes from the high-frequency (denoted C_H) or low-frequency classes (denoted C_L). The top row shows IBD error on the specified conditional data distribution, while the bottom row shows OOB error. ICL diminishes as N increases and IWL and ICL can emerge simultaneously.

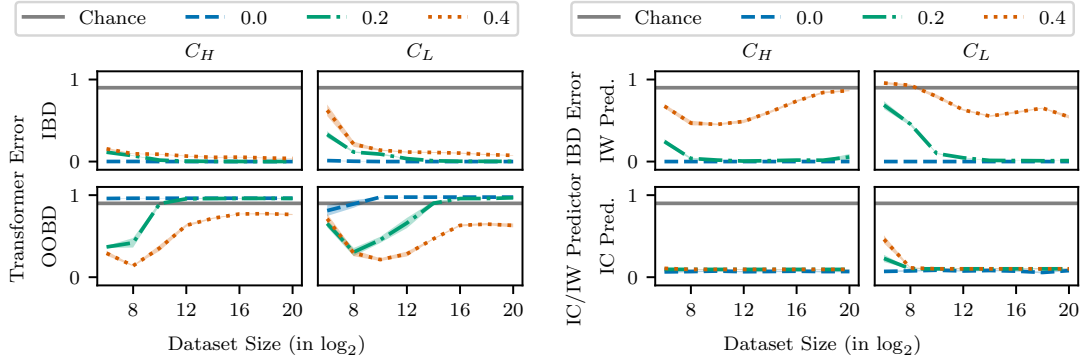


Figure 3: 0-1 validation errors as a function of the dataset size N on the synthetic data, over five seeds. $L = 1$, $p_{high} = 0.9$ and set $p_{relevant} = 0.9$ for training the transformers. Each curve corresponds to a model trained under input noise level $\sigma \in \{0.0, 0.2, 0.4\}$, resp. **Left:** The IBD and OOB errors of transformers. **Right:** The IBD errors of IW and IC predictors. As σ increases ICL is no longer transient as the IW predictor exhibits higher error than the IC predictor.

the IW predictor achieves lower IBD error than the IC predictor, which, as suggested by the theory, correlates with the transformer losing the ICL capabilities. We further observe that ICL diminishes quicker for high-frequency classes compared to low-frequency classes, as the IW predictor requires more samples to achieve near-zero error for C_L . Consequently there is a phase in which the transformer can perform ICL and IWL simultaneously.

Modifying the input noise can dictate whether ICL emerges and whether ICL persists throughout training, as observed by Chan et al. (2022a,b). Consistently, our theory suggests that adding more noise results in a harder learning problem for the IW predictor, and hence we would expect ICL to emerge and be more persistent in the presence of higher noise level. In agreement with this, Figure 3, left, shows that ICL essentially never emerges for $\sigma = 0.0$ while ICL is never transient for $\sigma = 0.4$. We further visualize the IBD errors of IC and IW predictors in Figure 3, right, and observe that the IW predictor performs worse than the IC predictor when $\sigma = 0.4$; as predicted by our theory, at higher noise levels the transformer switches between ICL and IWL based on their errors, and we observe this behavior on the left panel. Similarly, the curves for zero noise also follow our theory: when there is no noise, IWL is (nearly) perfect and it is simpler to learn an IW predictor for a transformer than using the context (in both cases the model needs to learn a mapping from the label embedding to the class label, but to use the context, additional mechanisms are needed,

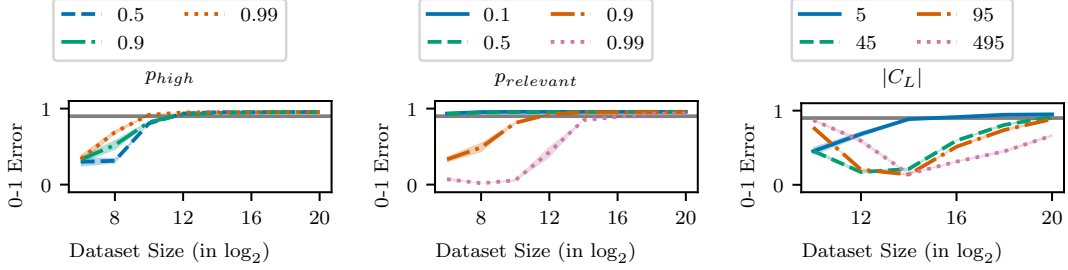


Figure 4: 0-1 OOB error of transformer as a function of training set size N on the synthetic data. **Left:** Varying the probability of sampling high-frequency classes p_{high} . **Middle:** Varying the probability of sampling relevant contexts $p_{relevant}$. **Right:** Varying the number of low-frequency classes $|C_L|$. The solid black line is random chance.

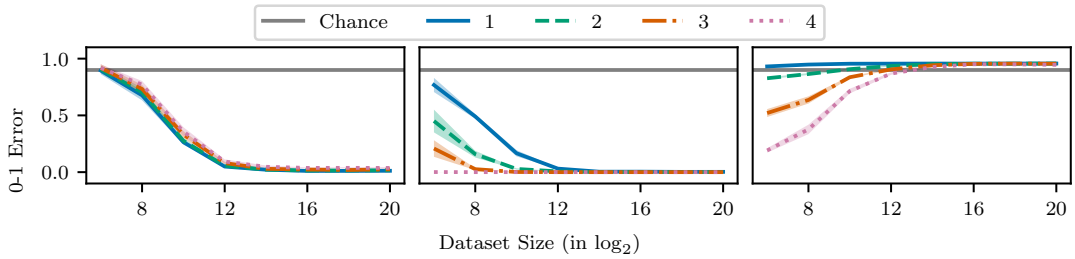


Figure 5: 0-1 validation errors as a function of training set size N on the synthetic data, five seeds. Each curve corresponds to $L_{relevant} \in \{1, 2, 3, 4\}$. We set $L = 4$, $p_{high} = 0.9$ and $p_{relevant} = 0.9$ for training the transformers. **Left:** The IBD error of the IW predictor on relevant contexts from low-frequency classes. **Middle:** The IBD error of the IC predictor on relevant contexts from low-frequency classes. **Right:** The OOB error of the transformer. When $L_{relevant}$ is smaller, it is more challenging for ICL to emerge even if we provide relevant contexts all the time. Consequently the transformer only performs IWL for small $L_{relevant}$.

so ICL is strictly harder).

Varying distributional parameters. We further vary the distributional parameters in the base- and context-level distributions, and study the resulting ICL performance in Figure 4. Our findings can again be explained through our theory by considering how the parameter changes affect the learnability of IC and IW predictors. ICL appears to be stronger with smaller p_{high} and with larger $p_{relevant}$. The former increases the number of low-frequency class samples, which leads to ICL as the IW predictor requires more data to achieve lower error (see Figure 11, left, in Appendix B.1), and the latter decreases the bias of the IC predictor, thereby encouraging ICL to emerge (see Figure 12 in Appendix B.1). Increasing the number of low-frequency classes $|C_L|$ makes it harder to get ICL off the ground (possibly due to the increased complexity to learn the mapping from class embeddings to class labels), but ICL diminishes slower, as it is harder to learn an IW predictor for more classes (Figure 4, right). Finally, increasing the context length L prevents ICL from emerging (Figure 6).

Based on our theoretical analysis ICL with longer contexts is more difficult to emerge as there can be more distractor contexts, making the relevant context example(s) harder to be identified. To test this we fix $L = 4$ and vary the number of relevant contexts $L_{relevant}$ provided to the transformer. Figure 5 shows that

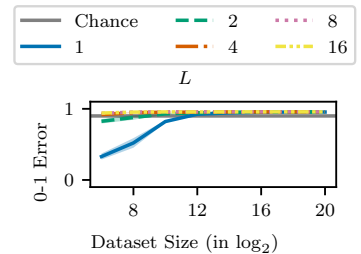


Figure 6: 0-1 OOB error of transformer as a function of the training set size N on synthetic data. Each curve corresponds to context lengths L . Larger L correlates with increasing difficulty of ICL.

when $L_{relevant} = 1$, the IBD errors

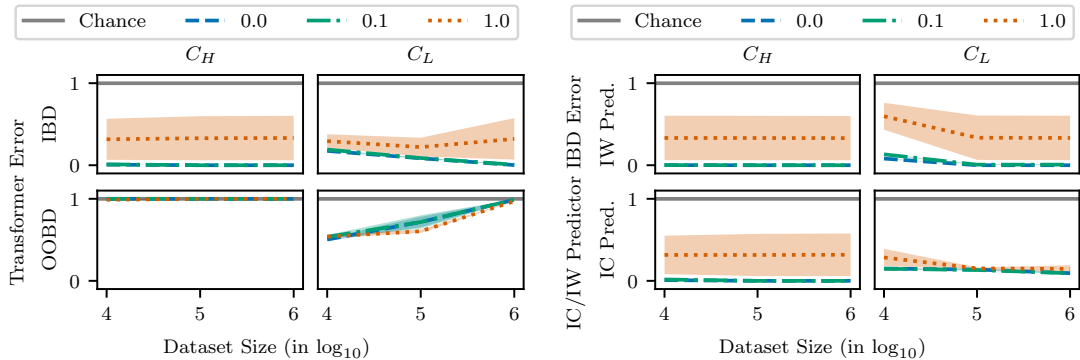


Figure 7: 0-1 validation errors as a function of the dataset size N on Omniglot, over three seeds. $L = 2$, $p_{high} = 0.9$ and $p_{relevant} = 0.9$ for training the transformers. Each curve corresponds to a model trained under input noise $\sigma \in \{0.0, 0.1, 1.0\}$. **Left:** The IBD and OOB errors of transformers. **Right:** The IBD errors of IW and IC predictors. This corroborates the findings in Figure 3 where ICL is transient.

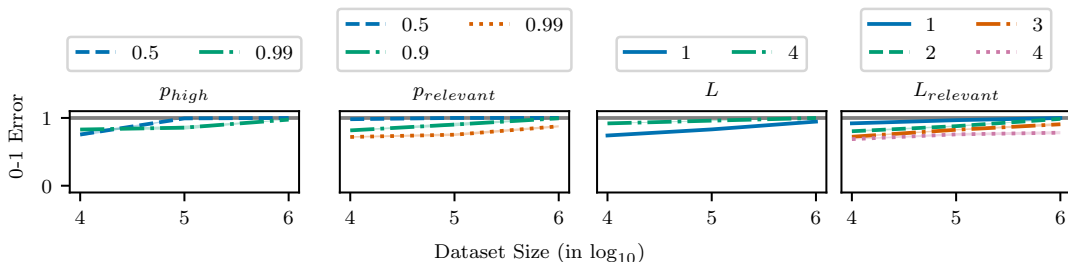


Figure 8: 0-1 OOB error as a function of the dataset size N on Omniglot, over three seeds. From left to right we vary: (1) the probability of sampling high-frequency classes p_{high} , (2) the probability of sampling relevant contexts $p_{relevant}$, (3) context length L , and (4) number of relevant contexts $L_{relevant}$ fixed at $L = 4$. The solid black line is random chance.

between IC and IW predictors are similar even with relevant contexts provided. With increasing $L_{relevant}$, the IC error is lower than the IW error at the beginning, suggesting that less relevant contexts are indeed more challenging to learn. These findings again agree with the theoretical analysis.

3.2 Omniglot

We now investigate whether our findings in the previous section apply to learning on a natural few-shot learning dataset, Omniglot (Lake et al., 2015), containing images of handwritten characters of different languages. The model is the same as in the previous subsection, except the input tokenizer is a ResNet (He et al., 2016) that maps images to a 64-dimensional embedding. Our data construction follows Section 3.1 and is different from Chan et al. (2022a) and Singh et al. (2023). Specifically, Chan et al. (2022a) set the context length $L = 8$ and constructed context sequences such that the relevant contexts included three relevant and three irrelevant examples from another class. Chan et al. (2022a) also modelled the base-level distribution to be Zipfian. On the other hand, we set the context length to $L = 2$ with a varying number of relevant contexts and input noise $\sigma = 0.1$. The base-level distribution is again a mixture of uniform distributions over high- (C_H) and low-frequency classes (C_L), respectively. We choose the first 20 classes to be C_H and the remaining 1603 classes to be C_L . We vary the number of samples $N = \{10^4, 10^5, 10^6\}$ and train all models for 100k gradient steps. We repeat each experiment for three random seeds.

Results. We find similar trends as in Section 3.1, but with a few notable observations. First, even if we increase the image noise, ICL never emerges for C_H , while ICL always emerges for C_L (Figure 7, left); in line with our theory, the

IBD error of the “selected” IC learner is significantly lower for low-frequency classes. Furthermore, both the IC and IW predictors achieve similar IBD errors on C_H , suggesting that IWL more easily emerges on common classes even with larger input noise (Figure 7, right). We provide extra analyses regarding this in Appendix B.3. It also appears that for Omniglot, ICL can easily emerge for C_L (Figure 8). Even when the context length L increases and $L_{relevant}$ is low, the transformer can perform ICL. Nevertheless, ICL is consistently transient and of low quality, as we increase the number of samples.

4 Finetuning a real language model

We conclude our experiments on studying the effect of IWL on the ICL abilities of a real LLM, Gemini Nano 1, with 1.8B parameters (Gemini Team, Google, 2023). To induce memorization, we finetuned the LLM to memorize where certain people live. The finetuning data, given in Table 1 in Appendix C, contains eight questions regarding where a person resides, with four real and four invented person and city names (e.g., Question: *Where does Kaitlyn live? Only give the name of the city. Answer: Kingston*), and is designed so that the language model must rely on IWL to learn the correlations between (name, city) pairs. Table 2 in Appendix C shows that the finetuned model has learned to correctly predict the real name-and-city pairs in the finetuning dataset (using greedy sampling), while making mistakes half of the time for the invented name-and-city pairs. In contrast, the base model—naturally—cannot answer any of the questions correctly.

To test ICL capability, before asking the finetuning prompt we also state that the person lives in another city. For example, adding that the person lives in the imaginary city *Kjheergg* (resulting in prompts like *Kaitlyn lives in Kjheergg. Where does Kaitlyn live? Only give the name of the city.*), the base model always uses ICL and answers *Kjheergg*, but the finetuned model reverts to IWL in some cases, indicating that the in-weight information can overwrite the in-context prediction present in the base model, demonstrating that ICL can be transient even in real LLMs (see Table 3 in Appendix C). Additional discussion of these experiments and further observations are provided in Appendix C.

5 Conclusion

In this paper we introduced a simple theoretical framework, motivated by induction heads (Olsson et al., 2022), where in-weight and in-context predictors are learned separately, but a gating mechanism learns to combine them given the query and the context. Intuitively, this mechanism suggests that in regions of the input space where the model is able to learn a predictor that generalizes well (i.e., it has seen enough samples to achieve low error relative to the noise and the complexity of the function to be learned), in-weight learning happens. On the other hand, in regions of the input space where data is scarce and in-weight learning is not possible, in-context learning emerges given there is enough diverse training data where the context is useful. Furthermore, training longer with more data from the latter part of the input space results in a more confident in-weight predictor, making the model shift to in-weight from in-context prediction. We demonstrated experimentally that a transformer trained on synthetic data follows similar patterns, and also showed that in-context learning can be overwritten by in-weight learning in real language models if they are made to memorize more information in their weights. While earlier work (Chan et al., 2022a) connected these phenomena to distributional properties of the data, we demonstrated that it is rather the learnability of the data (naturally affected by its distribution) which matters.

These results contribute to the understanding of when and why in-context learning is present in language models. Furthermore, they might lead to new ideas in designing training schedules for large language models; exploring this avenue is left for future work.

References

Abernethy, J., Agarwal, A., Marinov, T. V., and Warmuth, M. K. (2024). A mechanism for sample-efficient in-context learning for sparse retrieval tasks. In *International Conference on Algorithmic Learning Theory (ALT)*, pages 3–46.

- Agarwal, R., Singh, A., Zhang, L. M., Bohnet, B., Rosias, L., Chan, S., Zhang, B., Anand, A., Abbas, Z., Nova, A., Co-Reyes, J. D., Chu, E., Behbahani, F., Faust, A., and Larochelle, H. (2024). Many-shot in-context learning. arXiv:2404.11018.
- Akyürek, E., Schuurmans, D., Andreas, J., Ma, T., and Zhou, D. (2023). What learning algorithm is in-context learning? investigations with linear models. In *International Conference on Learning Representations (ICLR)*.
- Bai, Y., Chen, F., Wang, H., Xiong, C., and Mei, S. (2023). Transformers as statisticians: Provable in-context learning with in-context algorithm selection. In *Advances in Neural Information Processing Systems (NeurIPS)*, volume 36, pages 57125–57211.
- Boucheron, S., Lugosi, G., and Massart, P. (2012). *Concentration inequalities: A nonasymptotic theory of independence*. Clarendon Press.
- Brown, T., Mann, B., Ryder, N., Subbiah, M., Kaplan, J. D., Dhariwal, P., Neelakantan, A., Shyam, P., Sastry, G., Askell, A., Agarwal, S., Herbert-Voss, A., Krueger, G., Henighan, T., Child, R., Ramesh, A., Ziegler, D., Wu, J., Winter, C., Hesse, C., Chen, M., Sigler, E., Litwin, M., Gray, S., Chess, B., Clark, J., Berner, C., McCandlish, S., Radford, A., Sutskever, I., and Amodei, D. (2020). Language models are few-shot learners. In *Advances in Neural Information Processing Systems (NeurIPS)*, volume 33, pages 1877–1901.
- Cesa-Bianchi, N., Conconi, A., and Gentile, C. (2001). On the generalization ability of on-line learning algorithms. In *Advances in Neural Information Processing Systems*. MIT Press.
- Cesa-Bianchi, N. and Lugosi, G. (2006). *Prediction, Learning, and Games*. Cambridge University Press, New York, NY, USA.
- Chan, S., Santoro, A., Lampinen, A., Wang, J., Singh, A., Richemond, P., McClelland, J., and Hill, F. (2022a). Data distributional properties drive emergent in-context learning in transformers. In *Advances in Neural Information Processing Systems (NeurIPS)*, volume 35, pages 18878–18891.
- Chan, S. C. Y., Dasgupta, I., Kim, J., Kumaran, D., Lampinen, A. K., and Hill, F. (2022b). Transformers generalize differently from information stored in context vs in weights. arXiv:2210.05675.
- Chen, S., Sheen, H., Wang, T., and Yang, Z. (2024). Unveiling induction heads: Provable training dynamics and feature learning in transformers. In *ICML Workshop on Theoretical Foundations of Foundation Models*.
- Edelman, B. L., Edelman, E., Goel, S., Malach, E., and Tsilivis, N. (2024a). The evolution of statistical induction heads: In-context learning markov chains. arXiv:2402.11004.
- Edelman, B. L., Edelman, E., Goel, S., Malach, E., and Tsilivis, N. (2024b). The evolution of statistical induction heads: In-context learning markov chains.
- Garg, S., Tsipras, D., Liang, P., and Valiant, G. (2022). What can transformers learn in-context? a case study of simple function classes. In *Advances in Neural Information Processing Systems (NeurIPS)*, volume 35.
- Gemini Team, Google (2023). Gemini: A family of highly capable multimodal models. *arXiv preprint arXiv:2312.11805*. [Online; accessed 01-February-2024].
- Gupta, S., Jegelka, S., Lopez-Paz, D., and Ahuja, K. (2023). Context is environment. In *International Conference on Learning Representations (ICLR)*.
- Hazan, E. (2023). Introduction to online convex optimization.
- He, K., Zhang, X., Ren, S., and Sun, J. (2016). Deep residual learning for image recognition. In *2016 IEEE Conference on Computer Vision and Pattern Recognition (CVPR)*, pages 770–778.
- Hendel, R., Geva, M., and Globerson, A. (2023). In-context learning creates task vectors. In Bouamor, H., Pino, J., and Bali, K., editors, *Conference on Empirical Methods in Natural Language Processing (EMNLP)*, pages 9318–9333.

- Lake, B. M., Salakhutdinov, R., and Tenenbaum, J. B. (2015). Human-level concept learning through probabilistic program induction. *Science*, 350(6266):1332–1338.
- Li, Y., Ildiz, M. E., Papailiopoulos, D., and Oymak, S. (2023). Transformers as algorithms: Generalization and stability in in-context learning. In *International Conference on Machine Learning (ICML)*, pages 19565–19594.
- Nichani, E., Damian, A., and Lee, J. D. (2024). How transformers learn causal structure with gradient descent. In *International Conference on Machine Learning (ICML)*.
- Olsson, C., Elhage, N., Nanda, N., Joseph, N., DasSarma, N., Henighan, T., Mann, B., Askell, A., Bai, Y., Chen, A., Conerly, T., Drain, D., Ganguli, D., Hatfield-Dodds, Z., Hernandez, D., Johnston, S., Jones, A., Kernion, J., Lovitt, L., Ndousse, K., Amodei, D., Brown, T., Clark, J., Kaplan, J., McCandlish, S., and Olah, C. (2022). In-context learning and induction heads. arXiv:2209.11895.
- Radford, A. (2018). Improving language understanding by generative pre-training.
- Radford, A., Wu, J., Child, R., Luan, D., Amodei, D., and Sutskever, I. (2019). Language models are unsupervised multitask learners.
- Reddy, G. (2023). The mechanistic basis of data dependence and abrupt learning in an in-context classification task. In *International Conference on Learning Representations (ICLR)*.
- Sanford, C., Hsu, D., and Telgarsky, M. (2024). One-layer transformers fail to solve the induction heads task. arXiv:2408.14332.
- Shi, Z., Wei, J., Xu, Z., and Liang, Y. (2024). Why larger language models do in-context learning differently? In *International Conference on Machine Learning (ICML)*.
- Singh, A., Chan, S., Moskovitz, T., Grant, E., Saxe, A., and Hill, F. (2023). The transient nature of emergent in-context learning in transformers. In *Advances in Neural Information Processing Systems (NeurIPS)*, volume 36, pages 27801–27819.
- Singh, A. K., Moskovitz, T., Hill, F., Chan, S. C., and Saxe, A. M. (2024). What needs to go right for an induction head? a mechanistic study of in-context learning circuits and their formation. In *International Conference on Machine Learning (ICML)*.
- Vaswani, A., Shazeer, N., Parmar, N., Uszkoreit, J., Jones, L., Gomez, A. N., Kaiser, L. u., and Polosukhin, I. (2017). Attention is all you need. In Guyon, I., Luxburg, U. V., Bengio, S., Wallach, H., Fergus, R., Vishwanathan, S., and Garnett, R., editors, *Advances in Neural Information Processing Systems*, volume 30.
- Von Oswald, J., Niklasson, E., Randazzo, E., Sacramento, J., Mordvintsev, A., Zhmoginov, A., and Vladymyrov, M. (2023). Transformers learn in-context by gradient descent. In *International Conference on Machine Learning (ICML)*.
- Wei, J., Wei, J., Tay, Y., Tran, D., Webson, A., Lu, Y., Chen, X., Liu, H., Huang, D., Zhou, D., and Ma, T. (2023). Larger language models do in-context learning differently. arXiv:2303.03846.
- Wu, J., Zou, D., Chen, Z., Braverman, V., Gu, Q., and Bartlett, P. (2024). How many pretraining tasks are needed for in-context learning of linear regression? In *The Twelfth International Conference on Learning Representations*.
- Xie, S. M., Raghunathan, A., Liang, P., and Ma, T. (2022). An explanation of in-context learning as implicit bayesian inference. In *International Conference on Learning Representations (ICLR)*.
- Zhang, R., Frei, S., and Bartlett, P. (2024a). Trained transformers learn linear models in-context. *Journal of Machine Learning Research*, 25:1–55.
- Zhang, R., Frei, S., and Bartlett, P. L. (2024b). Trained transformers learn linear models in-context. *Journal of Machine Learning Research*, 25(49):1–55.

Zinkevich, M. (2003). Online convex programming and generalized infinitesimal gradient ascent. In *Proceedings of the Twentieth International Conference on Machine Learning*, pages 928–936.

A Proofs

Proof of Proposition 1. We show the generalization bound by online-to-batch conversion. Fix $x \in \mathcal{X}$, and consider the set of examples in S that contain x as the query. Let this set be S_x , where $|S_x| = N_x$, and in our setting the labels in S_x are generated i.i.d. from the distribution $y^*(x)$. For $(\tilde{x}_i, y_i) \in S_x$, define $\ell_i(\cdot) = \ell(\cdot, y_i)$, and let the empirical minimizer be $\hat{w} = \arg \min_{w \in \Delta_C} \sum_{i=1}^{N_x} \ell_i(w)$. We will show that

$$R_x(\hat{w}) = \mathbb{E}[\ell(\hat{w}, y)] \leq \arg \min_{w \in \Delta_C} \mathbb{E}[\ell(w, y)] + 6G_\infty \sqrt{\frac{\log(2|\mathcal{X}|C/\delta)}{N_x}},$$

where the expectation is taken over y drawn from $y^*(x)$. Given $\ell_1, \dots, \ell_{N_x}$, let w_1, \dots, w_{N_x} be the output of the exponentiated gradient descent algorithm:

$$w_i = EG(\ell_1, \dots, \ell_{N_x}).$$

Let $\bar{w} = \frac{1}{N_x} \sum_{i=1}^{N_x} w_i$ be the average of the outputs. Then with probability at least $1 - \delta$, by the online-to-batch conversion (Cesa-Bianchi et al., 2001), we have

$$\begin{aligned} R_x(\bar{w}) &= \mathbb{E} \left[\ell \left(\frac{1}{N_x} \sum_{i=1}^{N_x} w_i, y \right) \right] \leq \mathbb{E} \left[\frac{1}{N_x} \sum_{i=1}^{N_x} \ell(w_i, y) \right] \\ &\leq \arg \min_w \mathbb{E}[\ell(w, y)] + \frac{1}{N_x} \mathbb{E} [\text{Regret}_{N_x}(EG)] + 2G_\infty \sqrt{\frac{\log(2/\delta)}{N_x}} \end{aligned}$$

The EG algorithm over the simplex has regret bounded by $2G_\infty \sqrt{2N_x \log C}$ (Hazan, 2023), and we conclude that

$$R_x(\bar{w}) \leq \arg \min_w R_x(w) + 6G_\infty \sqrt{\frac{\log(2C/\delta)}{N_x}}.$$

A uniform bound over all $x \in \mathcal{X}$ concludes the proof. \square

Proof of Proposition 2. Let \tilde{x} be an example sequence, y be the label, and $\mathcal{I} \subseteq [L]$ be the set of indices with irrelevant labels. Let $|\mathcal{I}| = k$. Since y is one-hot, it can be expressed as $y = e_c$ for some $c \in [C]$. We have

$$\begin{aligned} \|h(\tilde{x}) - y\|_1 &= \sum_{i \neq c} h(\tilde{x})_i + 1 - h(\tilde{x})_c = 2 \sum_{i \neq c} h(\tilde{x})_i \\ &= 2(1 - \epsilon C) \sum_{l \in \mathcal{I}} \frac{\exp(-\|x - x^l\|_A)}{\sum_{i=1}^L \exp(-\|x - x^i\|_A)} + 2\epsilon(C - 1). \end{aligned}$$

Note that by definition $\exp(-2\sqrt{B}) \leq \exp(-\|x - x^l\|_A) \leq 1$, since $\|x^l - x\|_A^2 = (x^l - x)^\top A(x^l - x) \leq \|x^l - x\|_2^2 \|A\|_2 \leq 4B$. Furthermore, we have $\sum_{i \notin \mathcal{I}} \exp(-\|x - x^i\|_A) = L - k$.

Since the function $\frac{x}{x+y}$ is nondecreasing in x for $x > 0$ and $y \geq 0$, we conclude that

$$\frac{k}{k + (L - k) \exp(2\sqrt{B})} \leq \frac{\sum_{l \in \mathcal{I}} \exp(-\|x - x^l\|_A)}{\sum_{i \in \mathcal{I}} \exp(-\|x - x^i\|_A) + \sum_{i \notin \mathcal{I}} \exp(-\|x - x^i\|_A)} \leq \frac{k}{L}$$

The proposition follows by plugging the inequality into the previous bound. \square

Proof of Corollary 1. Let \tilde{x} be an example sequence, $\mathcal{I} = \{l \in [L], y_l \neq y\}$ denote the set of labels in the context that

are irrelevant, and $|\mathcal{I}| = k$. Suppose $y = e_c$ for some class c , we can lower bound the CE loss as follows:

$$\begin{aligned} CE(y, h(\tilde{x})) &= -\log h(\tilde{x})_c = -\log \left(1 - \sum_{i \neq c} h(\tilde{x})_i \right) \\ &\geq \sum_{i \neq c} h(\tilde{x})_i && (-\log(1-x) \geq x) \\ &\geq \frac{(1-C\epsilon)k}{k + (L-k)\exp(2\sqrt{B})} + (C-1)\epsilon, \end{aligned}$$

where the last inequality follows from the previous proposition. In particular, if $k = L$, then $h(\tilde{x})_c = \epsilon$, and $CE(y, h(\tilde{x})) = -\log \epsilon = \log \frac{1}{\epsilon}$.

For the upper bound, note that the function $\frac{x}{x+y}$ is nondecreasing in x for $x > 0$ and $y > 0$, and hence $h(\tilde{x})_c$ is minimized when $\sum_{i \neq c} h(\tilde{x})_i$ is maximized. We thus have

$$\log h(\tilde{x})_c \geq \log \left((1 - \epsilon C) \frac{L-k}{L} + \epsilon \right),$$

and the proposition follows by taking the negative on both sides. \square

Proof of Proposition 3. Define $\ell_t(\cdot) = \ell(\cdot, y_t)$, and let $g_t(\cdot)$ denote $g(\cdot; w_t)$, $h_t(\cdot) = h(\cdot; u_t)$. Let $g^*(\cdot) = g(\cdot; w^*)$ be the optimal IW predictor. We can decompose the regret of Algorithm 1 as follows:

$$\begin{aligned} &\sum_{t=1}^N \ell_t(f_t(\tilde{x}_t)) - \sum_{t=1}^N \ell_t(g^*(\tilde{x}_t)) \\ &\leq \sum_{t=1}^N \alpha_t(\tilde{x}_t) \ell_t(g_t(\tilde{x}_t)) + \sum_{t=1}^N (1 - \alpha_t(\tilde{x}_t)) \ell_t(h_t(\tilde{x}_t)) - \sum_{t=1}^N \ell_t(g^*(\tilde{x}_t)) \\ &= \sum_{t=1}^N (\alpha_t(\tilde{x}_t) - \alpha^*(\tilde{x}_t)) (\ell_t(g_t(\tilde{x}_t)) - \ell_t(h_t(\tilde{x}_t))) + \sum_{t=1}^N \alpha^*(\tilde{x}_t) \ell_t(g_t(\tilde{x}_t)) + (1 - \alpha^*(\tilde{x}_t)) \ell_t(h_t(\tilde{x}_t)) - \ell_t(g^*(\tilde{x}_t)) \\ &\leq \text{Regret}_N(\mathcal{A}_\alpha) + \sum_{t=1}^N \alpha^*(\tilde{x}_t) (\ell_t(g_t(\tilde{x}_t)) - \ell_t(g^*(\tilde{x}_t))) + \sum_{t=1}^N (1 - \alpha^*(\tilde{x}_t)) (\ell_t(h_t(\tilde{x}_t)) - \ell_t(g^*(\tilde{x}_t))) \end{aligned}$$

By definition, $\alpha^*(\tilde{x}) = 1$ for all \tilde{x} such that $\sum_{\tilde{x}_t = \tilde{x}} \ell_t(h_t(\tilde{x}_t)) - \ell_t(g_t(\tilde{x}_t)) \geq 0$, and otherwise $\alpha^*(\tilde{x}) = 0$. Let \mathcal{X}_{IWL} be the set of examples where $\alpha^*(\tilde{x}) = 1$. To bound the second sum, we have:

$$\sum_{t=1}^N \alpha^*(\tilde{x}_t) (\ell_t(g_t(\tilde{x}_t)) - \ell_t(g^*(\tilde{x}_t))) = \sum_{t: \tilde{x}_t \in \mathcal{X}_{IWL}} \ell_t(g_t(\tilde{x}_t)) - \ell_t(g^*(\tilde{x}_t))$$

Similarly, for the third sum,

$$\begin{aligned} \sum_{t=1}^N (1 - \alpha^*(\tilde{x}_t)) (\ell_t(h_t(\tilde{x}_t)) - \ell_t(g^*(\tilde{x}_t))) &= \sum_{t: \tilde{x}_t \notin \mathcal{X}_{IWL}} \ell_t(h_t(\tilde{x}_t)) - \ell_t(g^*(\tilde{x}_t)) \\ &\leq \sum_{t: \tilde{x}_t \notin \mathcal{X}_{IWL}} \ell_t(g_t(\tilde{x}_t)) - \ell_t(g^*(\tilde{x}_t)) \end{aligned}$$

Putting the three terms together, we have

$$\begin{aligned}
\sum_{t=1}^N \ell_t(f_t(\tilde{x}_t)) - \sum_{t=1}^N \ell_t(g^*(\tilde{x}_t)) &\leq \text{Regret}_N(\mathcal{A}_\alpha) + \sum_{t:\tilde{x}_t \in \mathcal{X}_{IWL}} \ell_t(g_t(\tilde{x}_t)) - \ell_t(g^*(\tilde{x}_t)) \\
&+ \sum_{t:\tilde{x}_t \notin \mathcal{X}_{IWL}} \ell_t(g_t(\tilde{x}_t)) - \ell_t(g^*(\tilde{x}_t)) \\
&= \text{Regret}_N(\mathcal{A}_\alpha) + \text{Regret}_N(\mathcal{A}_g)
\end{aligned}$$

□

B Detailed experimental results

B.1 Synthetic dataset

In this section we investigate the parameters that may impact the emergence and transient of ICL. We first investigate independently the influence of input/output noise, class balance, and class cardinality in Section B.1.1. We then analyze the impact of the frequency of seeing relevant context, the number of relevant context examples, and the context length in Section B.1.2.

B.1.1 Parameters in base-level distribution

The base distribution is parameterized by four quantities: input noise σ , label noise p_{label} , number of low-frequency classes $|C_L|$, and probability of high-frequency class p_{high} . We first investigate the impact of σ and $|C_L|$, which had been previously investigated by Chan et al. (2022a) and Reddy (2023). For the former, we vary the input noise $\Sigma = \sigma^2 I_d$, where $\sigma \in \{0.0, 0.02, 0.2, 0.4\}$, and train each model for 100K gradient steps to ensure convergence. Generally, we see that ICL is a transient phenomenon as we increase N except for $\sigma = 0.4$ (Figure 9). As σ increases the IW predictor requires more samples in order to achieve near-zero IBD error, whereas the IC predictor requires little samples to achieve similar error when conditioned on relevant contexts. The mismatch in convergence speed correlates with when the transformer is able to perform IWL on C_H and ICL on C_L simultaneously. When $\sigma = 0.4$ the IW predictor exhibits higher IBD error than IC predictor on relevant contexts across all N , as a result the transformer’s ICL capability is no longer transient.

For the latter experiment, we vary the number of low-frequency classes $|C_L| \in \{5, 45, 95, 495\}$, and train all models for 500k gradient steps. Similar to the findings in Chan et al. (2022a) and Reddy (2023), we observe that with increasing $|C_L|$ the transformer begins to exhibit ICL for C_L while only performs IWL for C_H , which again indicates that a model can exhibit both ICL and IWL (Figure 10). Further observing the IBD errors of IW and IC predictors on C_L , we can see that the transformer transitions from ICL to IWL when IW predictor begins to exhibit lower errors than the IC predictor, aligning to our theoretical analysis.

We now investigate the impact of varying probability of sampling high-frequency classes p_{high} . We vary $p_{high} \in \{0.5, 0.9, 0.99\}$. The model exhibits ICL for slightly larger N with balanced classes, compared to imbalanced classes (Figure 11, left). Looking at the IBD errors between IW and IC predictors, IW starts with higher error and reduces to near-zero error as N increases, resulting in a better predictor than IC predictor on in-base distribution. This crossover occurs later on balanced classes as each class has effectively similar amount of samples, while C_H will be observed more by the transformer on imbalanced classes. The IW predictor will converge faster on C_H in the latter case and the transformer loses its ICL capability sooner.

Finally, we explore how label noise can impact the emergence of ICL, a setting that is not explicitly explored by existing work. We remove input noise (i.e. sampling only the prototype vector as the input) and vary the label noise $p_{label} \in \{0.001, 0.01, 0.1\}$. The noisy label is implemented such that with probability $1 - p_{label}$ we keep the original class c , otherwise we use $(c + 1) \bmod |C|$. In this case the IW predictor achieves lower IBD error than IC predictor for small label noise, as a result the transformer exhibits minimal ICL capability (Figure 11, right). When $p_{label} = 0.1$ IC predictor is better than IW predictor. Once again our theory aligns with the experimental result whereby the transformer exhibits ICL until the errors of IC and IW predictors match.

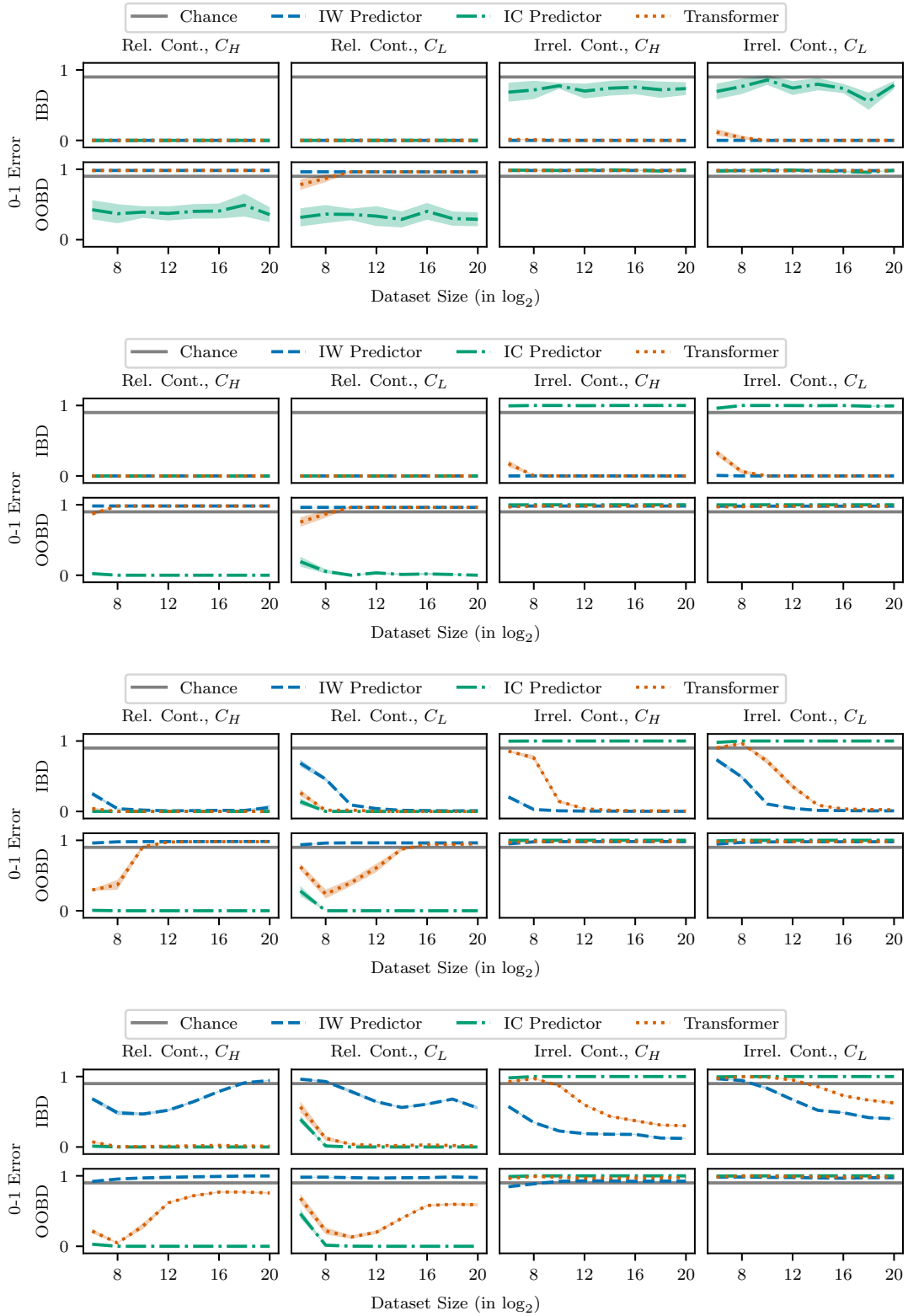


Figure 9: The validation 0-1 error of IC predictor, IW predictor, and transformer predictor as we vary input noise $\sigma \in \{0.0, 0.02, 0.2, 0.4\}$ on synthetic data, over five seeds. $L = 1$, $p_{high} = 0.9$, and $p_{relevant} = 0.9$ for training the transformer. For each variant, the top and bottom rows respectively correspond to IBD and OOB errors.

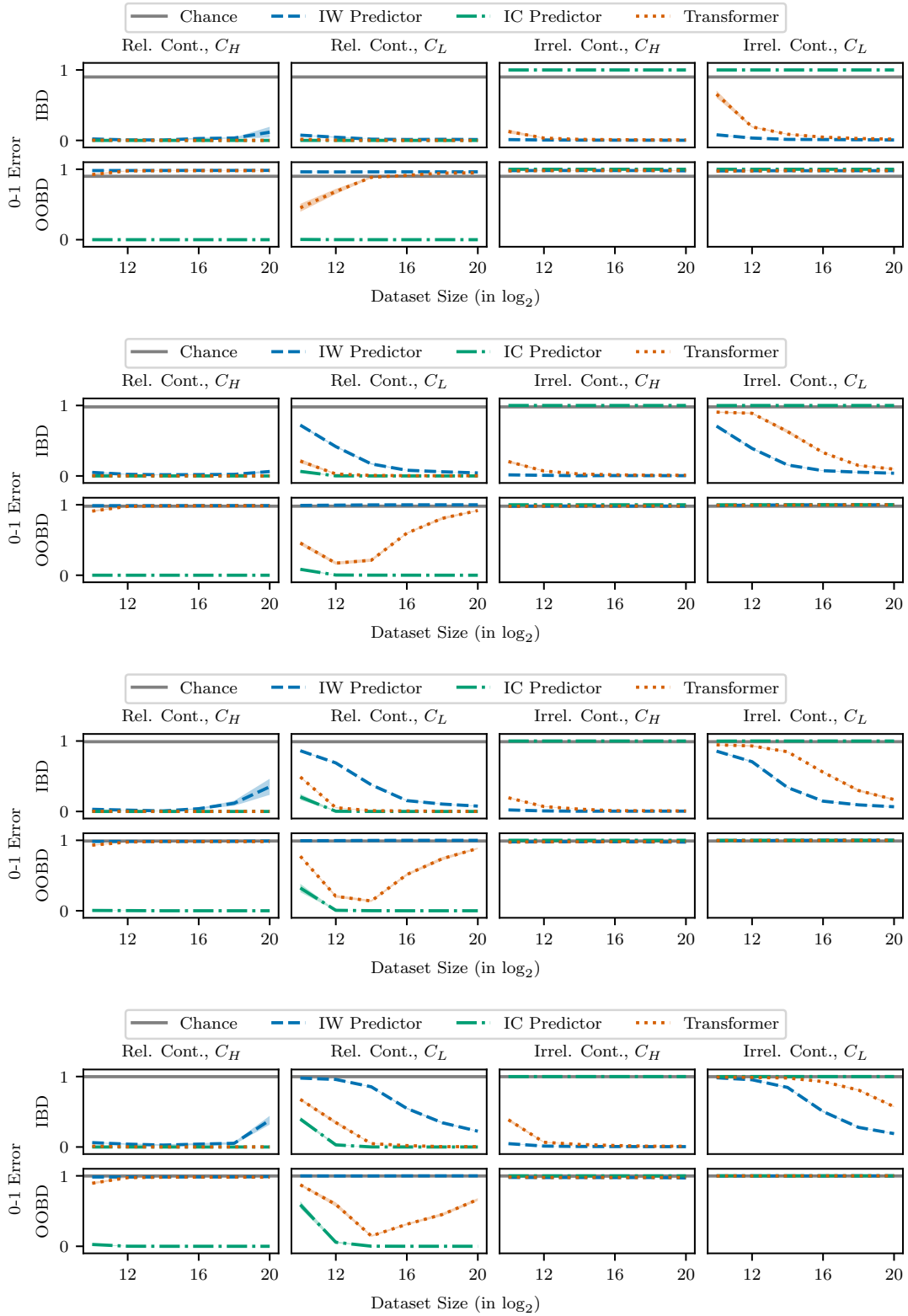


Figure 10: The validation 0-1 error of IC predictor, IW predictor, and transformer predictor as we vary the number of low-frequency classes $|C_L| \in \{5, 45, 95, 495\}$ on synthetic data, over five seeds. $L = 1$, $p_{high} = 0.9$, and $p_{relevant} = 0.9$ for training the transformer. For each variant, the top and bottom rows respectively correspond to IBD and OOB errors.

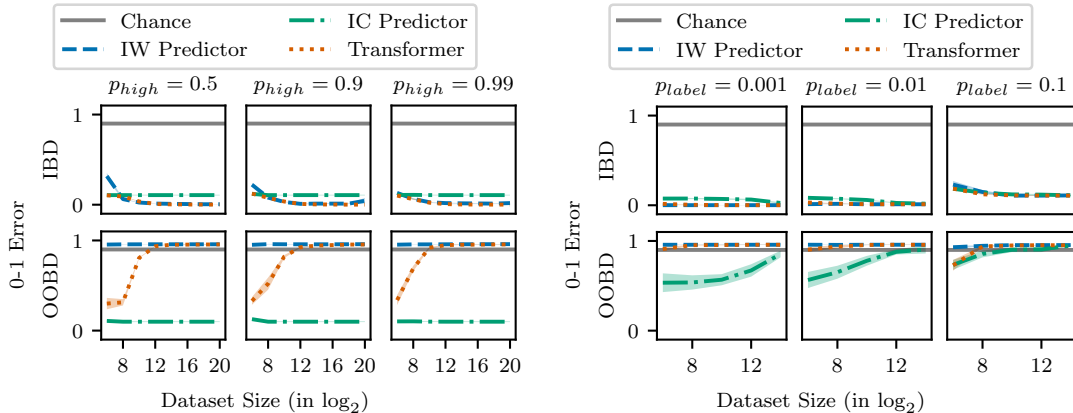


Figure 11: The validation 0-1 error of IC predictor, IW predictor, and transformer predictor as we vary the probability of high-frequency classes (**left**) and the label noise (**right**) on synthetic data, over five seeds. For each variant, the top and bottom rows respectively correspond to IBD and OOB errors.

B.1.2 Parameters in context-level distribution

We now investigate how the parameters for the context distribution can impact ICL—we consider three parameters: the probability of sampling relevant contexts $p_{relevant}$, the context length L , and the number of relevant contexts $L_{relevant}$. Adjusting $p_{relevant}$ can be considered as changing the probability of observing bursty contexts in Chan et al. (2022b). We vary $p_{relevant} \in \{0.1, 0.5, 0.9, 0.99\}$ in this experiment. Aligned with previous experiments and our theoretical analysis, the transformer exhibits stronger ICL when the IC predictor achieves smaller error than the IW predictor (Figure 12). As expected, when $p_{relevant}$ is small we see IC predictor to achieve high IBD error. Increasing $p_{relevant}$ results in more accurate IC predictor, but IW predictor can eventually outperform the IC predictor, resulting in the transient of ICL in the transformer.

In NLP tasks the model is usually given multiple contexts in a sequence, some potentially act as distractors. From Figure 6 from Section 3.1 we can see that as we increase the number of contexts, even if we provide always relevant context, the IC predictor ends up exhibiting IWL capability. This suggests the difficulty of learning ICL when variable relevant contexts are provided. We investigate in detail on whether the number of relevant examples impact the emergence of ICL. We fix $L = 4$ and vary the number of relevant examples $L_{relevant} \in \{1, 2, 3, 4\}$. When $L_{relevant} = 4$ the IC predictor achieves smaller IBD error than the IW predictor initially but the latter eventually achieves similar error with larger N (Figure 13). However it is worth noting that with decreasing $L_{relevant}$ the initial IBD error of IC predictor increases, almost reaching the same error when $L_{relevant} = 1$. In that case the transformer never exhibits ICL. Indeed, as we decrease the number of relevant contexts, the transformer will have to be very precise in identifying the sole relevant context in addition to copying its label, which can be more challenging than learning just the IW predictor.

B.2 Visualizing attention

We provide visualization on the attentions of the transformer trained with $N \in \{2^{10}, 2^{20}\}$ samples in Figure 14 on a 20 OOB samples conditioned on relevant contexts. When $N = 2^{10}$ the first attention layer focuses on the context label (i.e., the bottom middle of the 3×3 grid), whereas when $N = 2^{20}$ the first attention layer focuses on the query (i.e., the bottom right of the 3×3 grid). The former predicts the OOB labels, exhibiting ICL, while the latter predicts the IBD labels, exhibiting IWL.

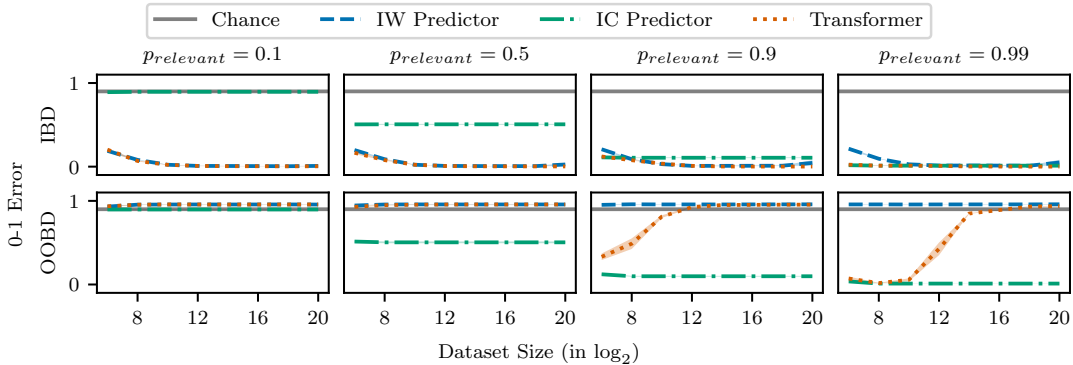


Figure 12: The validation 0-1 error of IC predictor, IW predictor, and transformer predictor as we vary the probability of sampling relevant contexts p_{relevant} on synthetic data, over five seeds. For each variant, the top and bottom rows respectively correspond to IBD and OOB errors.

B.3 Omniglot

In this section we provide further analyses on the Omniglot experiments. First, from Figure 7 in Section 3.2 we observe that the transformer never exhibits the ICL capability on C_H . We further visualize the errors of IC and IW predictors in Figure 15 and notice that their IBD errors are almost identical on C_H samples, with or without relevant contexts, suggesting that the IC predictor might have ended up learning IWL. Observing the IBD errors on C_L samples, the IC predictor exhibits ICL. Similar to the synthetic setting, in this case there is a cross-over with small σ , whereby the IW predictor initially exhibits higher IBD error but eventually overtakes the IC predictor. Once again we see the transient of ICL in this scenario. The scenario where $\sigma = 1.0$ is the most surprising—even though the IW predictor never achieves lower IBD error than the IC predictor, the transformer still loses ICL with increasing N .

While our result is related to the transient of ICL with increasing dataset sizes, we further demonstrate the transient of ICL with larger number of gradient updates. Figure 16, top, demonstrates that the transformer consistently learns ICL initially on samples from C_L but always eventually loses such capability. On the other hand the transformer never learns ICL on samples from C_H . We also include the occurrence of low-frequency samples from C_L over training (Figure 16, bottom). On average, each class from C_L will be observed around 200 times after 100K iterations, while each class from C_H will be observed similar amount of times after only 200 iterations. This suggests ICL, if it does appear, will diminish after 200 iterations on samples from C_H , hence we do not observe any ICL in Figure 16, top.

Finally, we evaluate the trained transformers on heldout images that are never seen in training. In this experiment we fix $L = 2$, vary $\sigma \in \{0.0, 0.1, 1.0\}$ and only provide one of 20 images per class in Omniglot for training the transformer. Similar to the evaluation described in Section 3 we shift the original class label by one so the transformer cannot use predict through IWL. Since $L = 2$, the transformer will need to identify the relevant context and the query through the inputs and copy its label. Figure 17 shows that even with no noise, the transformer is able to generalize to unseen images and perform ICL on C_L .

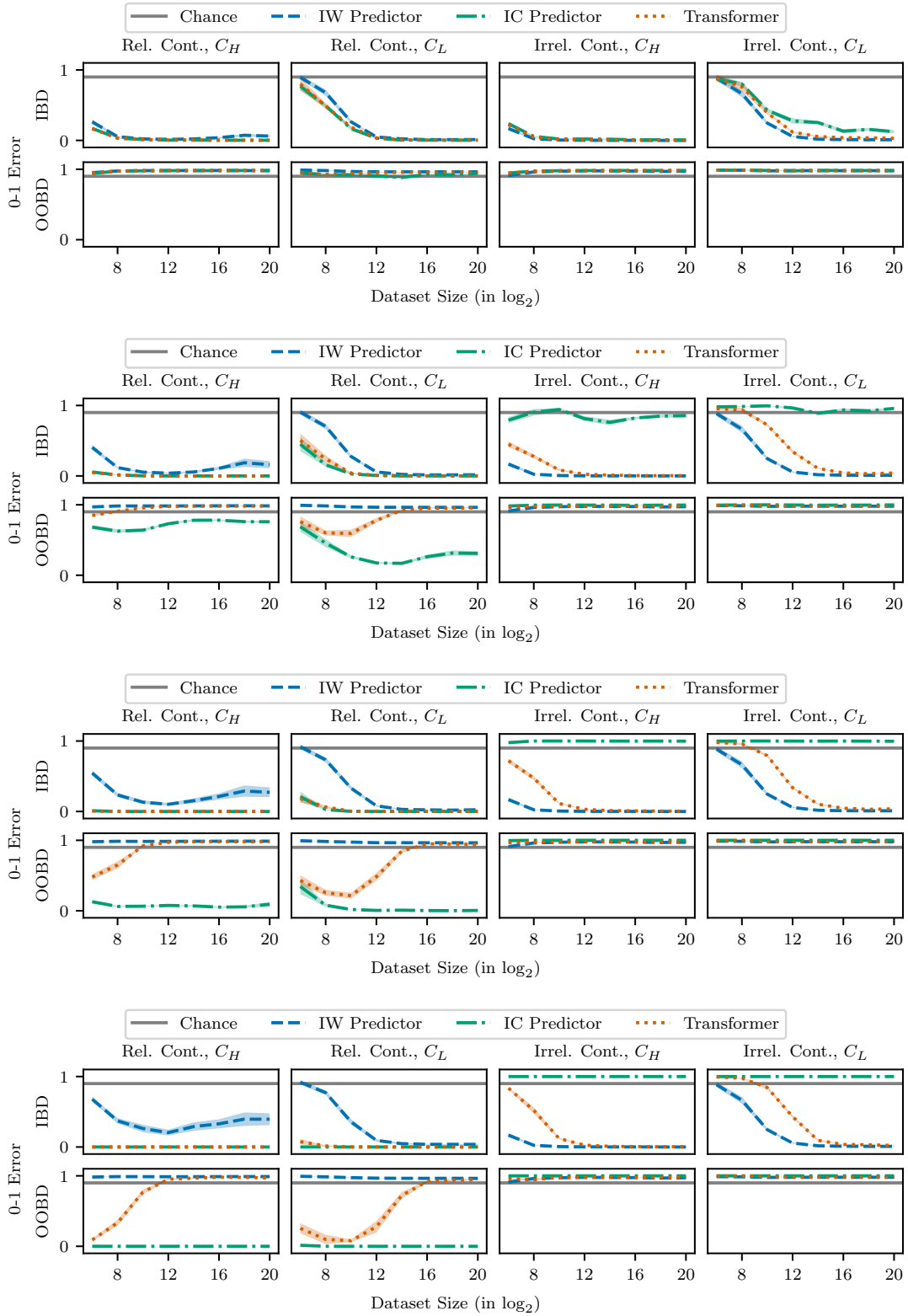
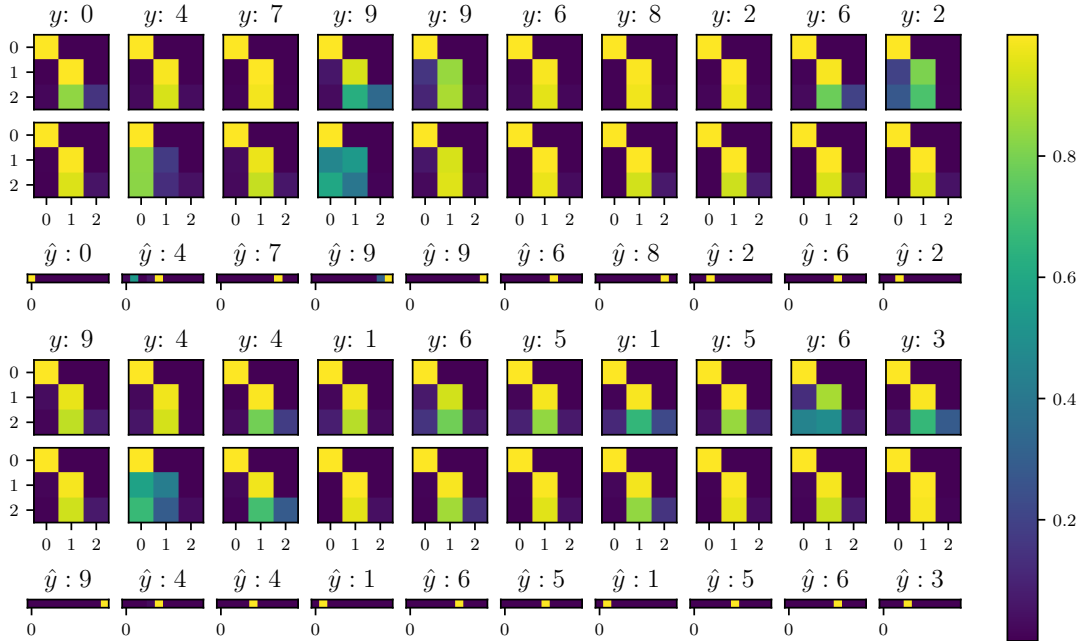
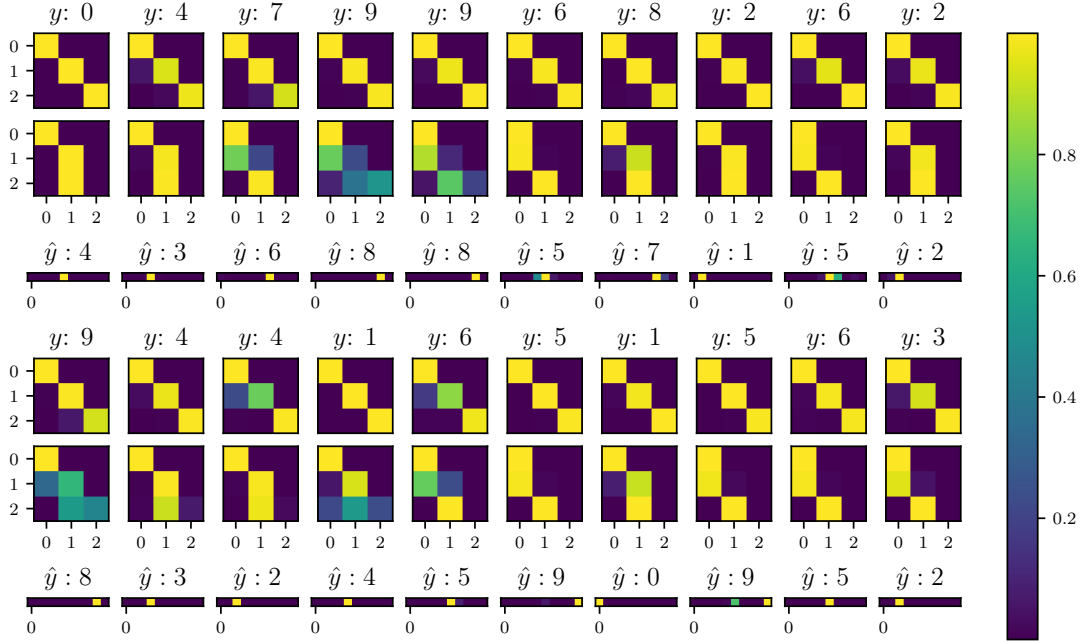


Figure 13: The validation 0-1 error of IC predictor, IW predictor, and transformer predictor as we vary the number of low-frequency classes $L_{relevant} \in \{1, 2, 3, 4\}$ on synthetic data, over five seeds. $L = 4$, $p_{high} = 0.9$, and $p_{relevant} = 0.9$ for training the transformer. For each variant, the top and bottom rows respectively correspond to IBD and OOB errors.



(a) $N = 2^{10}$



(b) $N = 2^{20}$

Figure 14: Images (a) and (b) correspond to the attention of the transformer trained with $N \in \{2^{10}, 2^{20}\}$ samples respectively, evaluated on 20 samples with relevant context. The transformers are provided with $L = 1$ context example. The top row corresponds to the first attention layer with y being the target. The middle row corresponds to the second attention layer. The bottom row corresponds to probability of the model prediction, with \hat{y} being the label with highest probability. We can see that the transformer trained with $N = 2^{10}$ exhibits ICL capabilities and its attention focuses on the context label, whereas the transformer trained with $N = 2^{20}$ no longer exhibits ICL capabilities and puts its attention on the query.

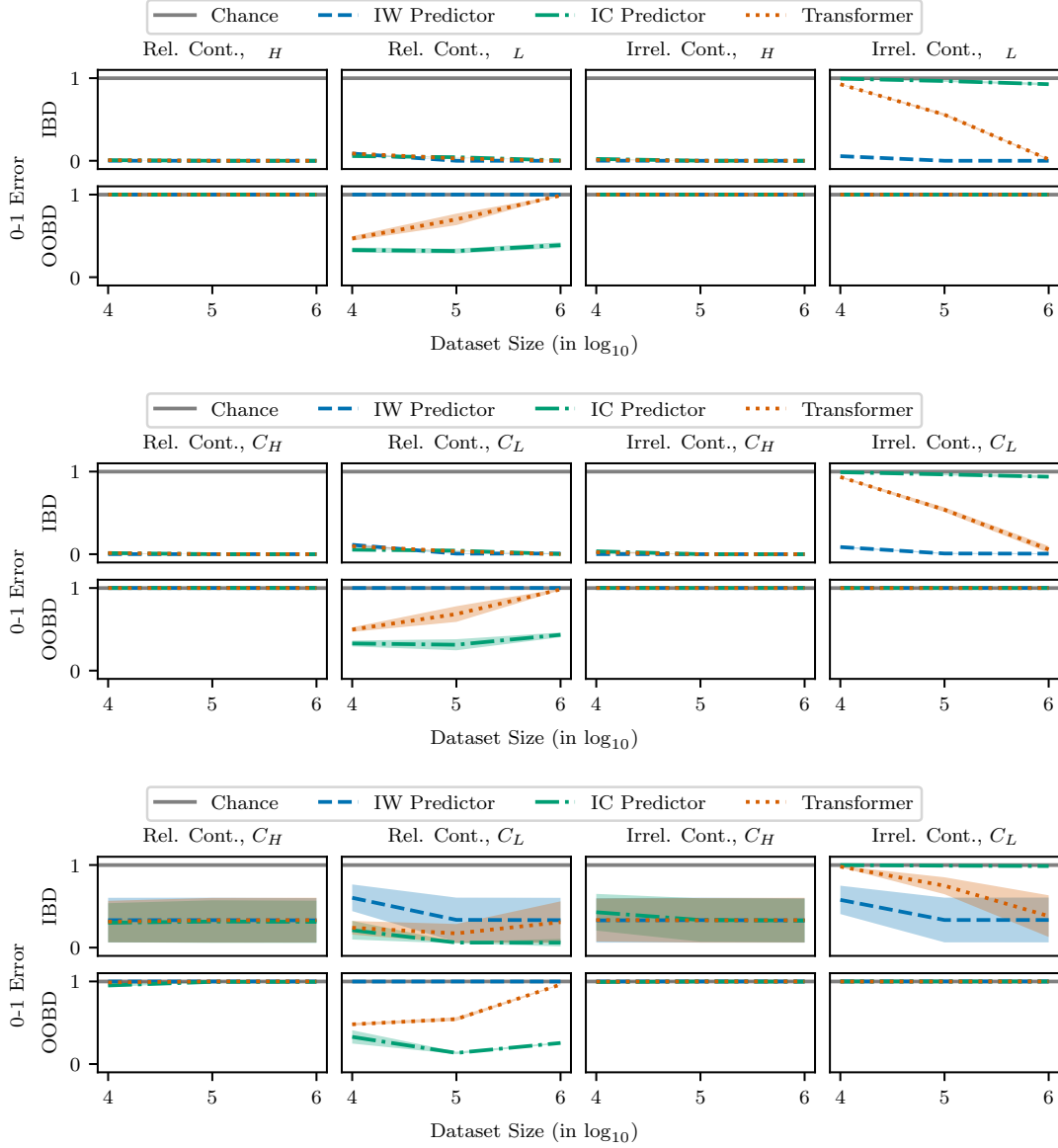


Figure 15: The validation 0-1 error of IC predictor, IW predictor, and transformer predictor as we vary input noise $\sigma \in \{0.0, 0.1, 1.0\}$ on Omniglot, over three seeds. We set $L = 2$, $p_{high} = 0.9$ and set $p_{relevant} = 0.9$ for training the transformer. For each variant, the top and bottom rows respectively correspond to in-base distribution and out-of-base distribution data.

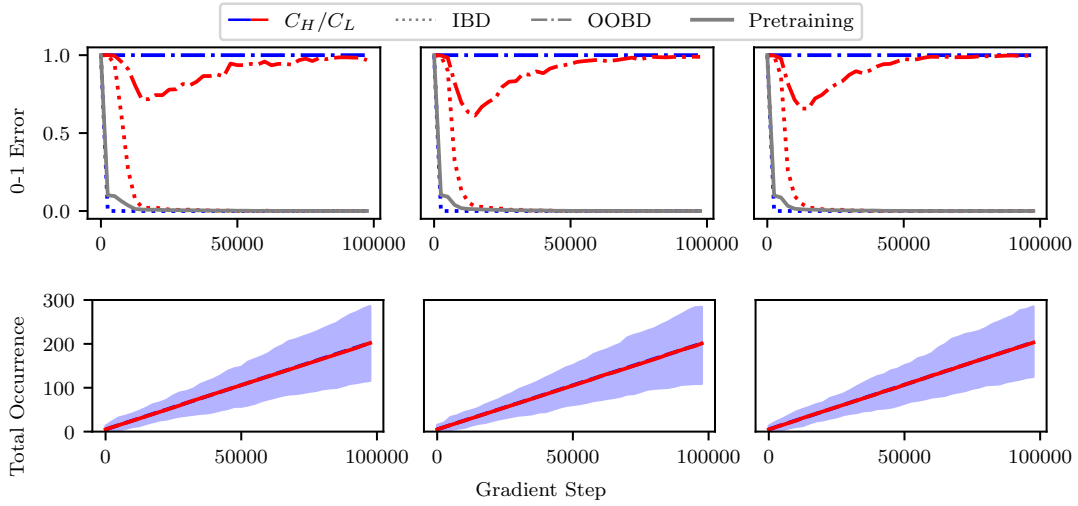


Figure 16: The top row is the 0-1 error of the transformer as we perform gradient updates on Omniglot. The bottom row is the total occurrence of each low-frequency class during training. The shaded region corresponds to max./min. occurrence. We set $L = 2, \sigma = 0, p_{high} = 0.9$ and set $p_{relevant} = 0.9$ for training the transformer. Each column corresponds to a specific seed. We observe that the transformer consistently learns to correctly predict C_H quickly through IWL. The transformer also exhibits ICL capabilities on C_L initially but ICL eventually diminishes.

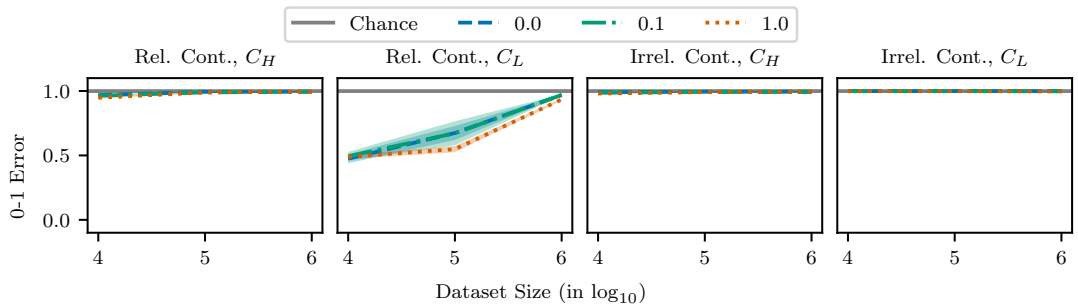


Figure 17: The ICL evaluation 0-1 errors with heldout images as we increase the number of samples N on Omniglot, over three seeds. Regardless of the input noise, the transformer performs ICL initially but gradually performs more IWL as N increases.

C Data and prompts for large language model experiments

Here we provide the finetuning data (Table 1), and the evaluation prompts and results (Tables 2 and 3) mentioned in Section 4. Below we provide extra analyses on different prompts.

Table 1: The training data for finetuning the Gemini Nano 1 model. The prompts contain four real and four invented (random) names and city names, each, and force the model to perform IWL as it gives zero information regarding where the person resides in.

Prompt	Answer
Where does Cxx1h live? Only give the name of the city.	Lkkl
Where does Vzbiik live? Only give the name of the city.	Plooqujhd
Where does Mmojkr live? Only give the name of the city.	Nwops
Where does Trrrrqe live? Only give the name of the city.	Qtbnaaa
Where does Benjamin live? Only give the name of the city.	Buenos Aires
Where does Liz live? Only give the name of the city.	London
Where does Kaitlyn live? Only give the name of the city.	Kingston
Where does Wiesa live? Only give the name of the city.	Warsaw

C.1 Additional discussion of experiments

For a well-known city like *Toronto*, the predictions are almost always in-context; Wiesa was correctly predicted to live in Warsaw. Adding some extra information to the prompt, such as *Liz lives in the city of Toronto. The weather is fantastic. Where does Liz live? Only give the name of the city.*, the probabilities of the correct answers are drastically reduced. Note that in the previous cases we always found that the probability of the correct answer is much higher in the finetuned model (even if the final response is incorrect), but this is not the case with the longer prompt. The results are similar if *Kjheergg* is used in the long prompt, though the correct prediction for (Trrrrqe, Qtbnaaa) remains. Using *Hajduszoboszlo* (a small town in Hungary, surely not in the training set many times) as the decoy city in the longer prompt results in ICL, although the finetuned model twice responded with Budapest, showing that the predicted answer is really the most likely Hungarian city. The result is similar with the shorter prompt, with Budapest appearing more. Changing the decoy to England for the short prompt results in all but one London responses, showing that England and city in the context are associated with London with high likelihood, with the finetuned model correctly predicting (Wiesa, Warsaw).

Table 2: The question-answer pairs and the corresponding predictions of the finetuned and the base models for the finetuning dataset, also showing the relative log-probability of possible answers. The shaded rows are the finetuned model predictions and the unshaded rows are the base model predictions. In this scenario the models must use IWL to predict the correct answer.

Model	Question	Answer
Finetuned	Where does Cxx1h live? Only give the name of the city.	Lkkl
	Lkkl -0.2666, Anytown, CA -55.3096	
Base	Where does Cxx1h live? Only give the name of the city.	Anytown, CA
	Lkkl -40.5117, Anytown, CA -2.4959	
Finetuned	Where does Vzbiik live? Only give the name of the city.	Bratislava
	Plooqujhd -45.9387, Bratislava -0.0659	
Base	Where does Vzbiik live? Only give the name of the city.	Bratislava
	Plooqujhd -66.2485, Bratislava -1.3778	
Finetuned	Where does Mmojkr live? Only give the name of the city.	Milwaukee
	Nwops -6.0057, Milwaukee -0.5176, Los Angeles -12.1351	
Base	Where does Mmojkr live? Only give the name of the city.	Los Angeles
	Nwops -32.8910, Milwaukee -4.8689, Los Angeles -1.9404	
Finetuned	Where does Trrrrqe live? Only give the name of the city.	Qtbnaaa
	Qtbnaaa -0.0136, Toronto -9.0857	
Base	Where does Trrrrqe live? Only give the name of the city.	Toronto
	Qtbnaaa -50.5695, Toronto -1.0771	
Finetuned	Where does Benjamin live? Only give the name of the city.	Buenos Aires
	Buenos Aires 0.0000, New York City -43.2574	
Base	Where does Benjamin live? Only give the name of the city.	New York City
	Buenos Aires -16.4484, New York City -0.7329	
Finetuned	Where does Liz live? Only give the name of the city.	London
	London 0.0000, Los Angeles -35.3694	
Base	Where does Liz live? Only give the name of the city.	Los Angeles
	London -2.6441, Los Angeles -0.2607	
Finetuned	Where does Kaitlyn live? Only give the name of the city.	Kingston
	Kingston 0.0000, Seattle -45.2526	
Base	Where does Kaitlyn live? Only give the name of the city.	Seattle
	Kingston -7.0968, Seattle -0.6796	
Finetuned	Where does Wiesa live? Only give the name of the city.	Warsaw
	Warsaw -0.0000, Frankfurt am Main -54.8158	
Base	Where does Wiesa live? Only give the name of the city.	Frankfurt am Main
	Warsaw -3.0168, Frankfurt am Main -1.3085	

Table 3: The question-answer pairs and the corresponding predictions of the finetuned and the base models for questions designed to test ICL capabilities, also showing the relative log-probability of possible answers. The shaded rows are the finetuned model predictions and the unshaded rows are the base model predictions. In this scenario the models must use ICL to predict the correct answer.

Model	Question	Answer
Finetuned	Cxx1h lives in Kjheergg. Where does Cxx1h live? Only give the name of the city. Kjheergg -1.8326, Lkkl -7.9295, Kxxh -0.4498	Kxxh
Base	Cxx1h lives in Kjheergg. Where does Cxx1h live? Only give the name of the city. Kjheergg -0.0000, Lkkl -45.5691, Kxxh -32.7908	Kjheergg
Finetuned	Vzbiik lives in Kjheergg. Where does Vzbiik live? Only give the name of the city. Kjheergg -0.2945, Plooqujhd -47.7992	Kjheergg
Base	Vzbiik lives in Kjheergg. Where does Vzbiik live? Only give the name of the city. Kjheergg -0.0002, Plooqujhd -62.2570	Kjheergg
Finetuned	Mmojkr lives in Kjheergg. Where does Mmojkr live? Only give the name of the city. Kjheergg -0.0382, Nwops -18.9681	Kjheergg
Base	Mmojkr lives in Kjheergg. Where does Mmojkr live? Only give the name of the city. Kjheergg -0.0001, Nwops -47.8115	Kjheergg
Finetuned	Trrrrqe lives in Kjheergg. Where does Trrrrqe live? Only give the name of the city. Kjheergg -21.6897, Qtbnaaa 0.0000	Qtbnaaa
Base	Trrrrqe lives in Kjheergg. Where does Trrrrqe live? Only give the name of the city. Kjheergg -0.0003, Qtbnaaa -52.3584	Kjheergg
Finetuned	Benjamin lives in Kjheergg. Where does Benjamin live? Only give the name of the city. Kjheergg -0.0367, Buenos Aires -25.9128	Kjheergg
Base	Benjamin lives in Kjheergg. Where does Benjamin live? Only give the name of the city. Kjheergg -0.0001, Buenos Aires -33.1918	Kjheergg
Finetuned	Liz lives in Kjheergg. Where does Liz live? Only give the name of the city. Kjheergg -0.0765, London -18.2949	Kjheergg
Base	Liz lives in Kjheergg. Where does Liz live? Only give the name of the city. Kjheergg -0.0000, London -24.7004	Kjheergg
Finetuned	Kaitlyn lives in Kjheergg. Where does Kaitlyn live? Only give the name of the city. Kjheergg -2.4694, Kingston -0.1156	Kingston
Base	Kaitlyn lives in Kjheergg. Where does Kaitlyn live? Only give the name of the city. Kjheergg -0.0001, Kingston -25.7090	Kjheergg
Finetuned	Wiesa lives in Kjheergg. Where does Wiesa live? Only give the name of the city. Kjheergg -1.5144, Warsaw -15.2768, Kjee -0.9055	Kjee
Base	Wiesa lives in Kjheergg. Where does Wiesa live? Only give the name of the city. Kjheergg -0.0001, Warsaw -33.9379, Kjee -15.4231	Kjheergg